The Effect of Velocity in Abrasive Waterjet Cutting – Efeito da Velocidade no Corte por Jacto de Água com Abrasivo

Dissertação apresentada para a obtenção do grau de Mestre em Engenharia Mecânica na Especialidade de Sistemas de Produção

Autor

João Pedro Morais Rodrigues Dias

Coordenadores
Professor Doutor Altino de Jesus Roque Loureiro
Professor Peter Bjurstam

Júri

Presidente	**Professora Doutora Marta Cristina Cardoso de Oliveira** **Professora Auxiliar da Universidade de Coimbra**
Vogais	**Professor Doutor José Domingos Moreira da Costa** **Professor Associado com agregação da Universidade de Coimbra** **Professor Doutor Altino de Jesus Roque Loureiro** **Professor Associado com agregação da Universidade de Coimbra** **Professora Doutora Cristina Maria Gonçalves dos Santos Louro** **Professora Auxiliar da Universidade de Coimbra**

Colaboração Institucional

Universidade Linkoping

Coimbra, Setembro, 2011

Agradecimentos

Em primeiro lugar gostaria de agradecer ao meu orientador, Professor Altino Loureiro pela infindável ajuda e disponibilidade. Aos meus Pais, pelo apoio incondicional. À Joana e ao Frankas pelas longas horas de conversas, desabafos e confissões. Ao Hugo, que me acompanhou nesta jornada sueca e pela sempre presente disponibilidade demonstrada. Ao Andrade pela companhia e hombridade sempre demonstrada.

Não me sendo possível numerar todos que me acompanharam durante todos estes anos, resta-me apenas congratular-me por possuir tal quantidade e qualidade de AMIGOS.

Por último, e que por inúmeras vezes o mais importante, um agradecimento especial e sentido à Mafalda.

A TODOS, manifesto a minha mais profunda gratidão.

Resumo

O presente trabalho teve por objectivo estudar a influência da velocidade e espessura de corte na qualidade, de cortes realizados por jacto de água com abrasivos. A qualidade da peça cortada é caracterizada através da rugosidade e ondulação da superfície de corte, do ângulo de afunilamento (Kerf Taper) e da largura do corte.

A rugosidade e ondulação foram medidas recorrendo a um rugosímetro. O ângulo de afunilamento foi analisado através de uma máquina de medição por coordenadas. A geometria do corte foi analisada com uma lente.

Os valores da rugosidade tendem a aumentar com a velocidade de corte e com a espessura. O aumento da velocidade de corte reduz a largura de corte, quer na face superior quer na base da chapa. A redução da espessura de corte reduz a rugosidade superficial do corte, mas aumenta o ângulo.

No final, são apresentadas algumas recomendações para reduzir o ângulo de afunilamento Kerf Taper bem como algumas considerações relevantes para a abordagem experimental de alguns problemas associados ao corte por jacto de água.

Palavra-chave: Corte por Jacto de água com abrasivo; Aço Carbono; Rugosidade; ângulo de afunilamento (Kerf Taper); Velocidade de corte; Espessura.

Abstract

In this thesis the influence of cutting velocity and thickness in workpieces cut with abrasive waterjet is analyzed.

The cut quality is characterized through the roughness and waviness from the cut surface, kerf taper angle and kerf width. Roughness and waviness was measured with a roughness machine. The kerf taper angle was measured using a coordinate measuring machine. Kerf geometry was analyzed with a magnifying lens.

Roughness values tend to increase with cutting speed and thickness. Increasing cutting speed reduces kerf width on top and bottom position, although kerf taper is increased.

In the Future Work chapter, some recommendation on how to reduce the kerf taper angle as well as considerations about experimental approach to some problems associated to the AWJ cutting are made.

Keywords: Abrasive Waterjet cutting (AWJ); Carbon Steel; Roughness; Kerf taper; Cutting Velocity; Thickness.

Index

Figure Index

Table Index

List of Acronyms

AJM   Abrasive Jet Machining

AWJ   Abrasive Water Jet

AWJM   Abrasive Water Jet Machine

CAA   Computer Aided Analyzes

CMM   Coordinate Measuring Machine

EDM   Electric Discharge Machining

PMC   Precision Coordinate Measuring Machine

Ra   Average Roughness

Rp   Peak Roughness

Rq   Root Mean Square Roughness

Rt   Total Roughness

Rv   Depth of the Deepest Valley

Ry   Maximum Roughness Height within a Sample Length

SRMI   Surface Roughness Measuring Instrument

UHP   Ultra High Pressure

UPMC   Ultra Precision Coordinate Machine

USM   Ultrasonic Machining

WJW   Waterjet Machining

1. Introduction

Waterjet technology is one of the fastest growing machine tool processes in the world due to its versatility and ease of operation, according to Folkes, J. (2009). The waterjet is a multitalented tool and can be used in applications such as cutting, drilling, milling and even cleaning and coating removal. It allows machining almost any material, such as metal, composites and rocks, and is able to compete side by side with other technologies, like plasma, laser and EDM wire.

By far the most common application is cutting. It is possible to cut just with water or with abrasives mixed into the flow.

Waterjet Machining (WJM) and Abrasive Waterjet Machining (AWJM) are two non-traditional or non-conventional machining processes. They belong to mechanical group of non-conventional processes like Ultrasonic Machining (USM) and Abrasive Jet Machining (AJM), following the Hascalik, A. *et al*. (2007) classification. Both processes, WJM and AWJM, share the same principle of functionality. Water flows from a pump, through plumbing and to a mixing tube where the abrasive particles coming from a reservoir tube are drained into the main flow, as illustrated in Fig 2.1-1, which was retrieved from http://www.omax.com and http://www.flowwaterjet.com website. At the mixing tube's end an orifice provides the cutting jet output.

Despite the simple system, it requires a number of extremely complex materials technologies, geometry and design.
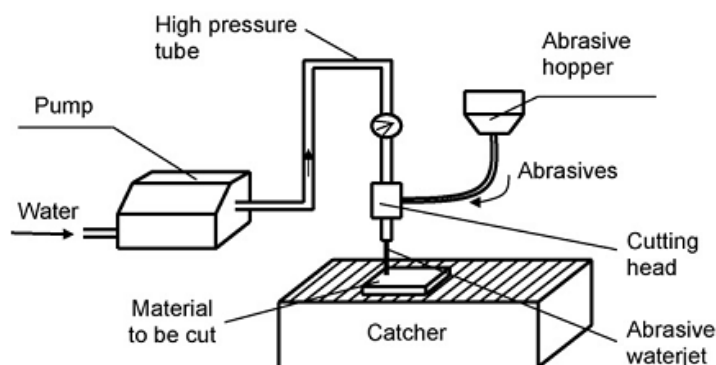
Fig 2.1-1 – Schematic of an abrasive waterjet cutting system

The main characteristics of the WJ technique are:

1. Extremely versatile process;
2. No heat affected zones;
3. No mechanical stresses;
4. Easy to program;
5. Thin material cutting;
6. Maximum cutting thickness of 254 mm;
7. Little material loss due to cutting;
8. Simple to fixture;
9. Low cutting forces;
10. One jet setup for nearly all abrasive jet jobs;
11. Quickly switch from pure waterjet to abrasive waterjet;
12. Little or no burr.

Despite all this characteristics, WJ and in this particularly case AWJ, holds some disadvantages important to mention.

An inappropriate selection of the cutting velocity may produce, on the cut surface, roughness values and kerf taper angles out of normal, according to Shanmugam, D. K. (2008). It may also influence the existence of burr, which would require secondary finishing. The existence of a material gap may produce cut surface defects. Each material has its own set of characteristics. The short life of some parts, like nozzle and orifice, add replacement costs and overheads to AWJ operation, according to Ness R., and Zibbell, R. (1996).

Another disadvantage is the fact that the cutting material is placed on top of support bars. This support bars may represent a problem in the final presentation of the work pieces, due to jet deflection.

The experimental work presented in this dissertation evaluates the effect of cutting velocity and plate thickness on the quality of waterjet cutting on carbon steel plates and is structured in six chapters.

In the next chapter, the state of the art is overviewed with references to some important parameters found in the AWJ system.

In chapter 3, the material used, the equipment and the operating procedure are referred. WJ machine, Surface Roughness Measuring Instrument (SRMI) and Coordinate

Measuring Machine (CMM) and magnifying lens are described as well as a brief description on how to program them. Descriptions on the geometries chosen are also made.

In chapter 4, the presentation and discussion of the results is presented with all the analysis made to the workpieces cut with AWJ.

In chapter 5, the conclusions drawn from the achieved results are presented, followed by closing remarks and future work orientation in chapter 6.

References follow on chapter 7, and chapter 8 encloses and appendix of data that complements the carried out study.

The experimental work presented in this dissertation was carried out on the Linköping University, Sweden.

2. State of the Art

This kind of technique requires a lot of background information. Only with a solid research is possible to investigate experimentally some of its parameters. In this chapter the water jet history, the global position in cutting processes and some of its most relevant parameters are mentioned, with greater emphasis on those that are being analyzed in this dissertation.

2.1. History

Waterjet cutting gain life in the 1950 by the hands of Dr. Norman Franz in a new attempt to transform sliced trees into lumber. He became the first person to study Ultra-High Pressure (UHP) as a cutting tool. He started by dropping heavy weights onto columns of water to force the water through a tiny orifice, this way short bursts of water under very high pressure, powerful enough to cut wood, were obtained, information retrieved from http://www.flowwaterjet.com. A lot of work and research has been done in this technique, aiming for better results in new materials to cut with less costs. One of the oldest goals in the entire life of the AWJ cutting system has been the elimination of the taper angle, by Shanmugam D. K. (2008).

2.2. Water Jet Cutting on the Market

Comparing to others techniques, like Laser, Plasma and wire EDM, WJ Cutting presents some advantages, according to Zheng, H. Y. *et al.* (1996) and Oliveira Santos, J. F. (1991). As said before waterjet is environmentally friendly and is a cold cutting process that eliminates slag deformation and dross waste, observed in Plasma and Laser cutting processes. Additionally, abrasive and water can be recycled. The flexibility and cold cutting characteristics of the waterjet make it an important tool for cutting applications of new materials such as composites and sandwiched materials that are difficult to machine with traditional machining processes, according to Wang, J. (1999). Abrasive waterjet is able to ignore many defect. Both plasma and laser cutting leave behind a heavy crust that is extremely difficult to remove, according to Akkurt A. *et al*. (2004). AWJ produces clean slits of higher quality than those produced by CO_2 laser beam, by Wang, J. and Wong, W.

C. K. (1999). AWJ is not only very important in metal material, for cutting composites it reveals to be a very useful machining process, according to. Shanmugam, D. K. (2002)

2.3. AWJ Parameters

One major problem found in this kind of technique is the amount of parameters that can influence positive or negatively the cut characteristics.

Parameter that can influence the cut:

- Cutting speed;
- Plate thickness;
- Water pressure;
- Size and abrasive flow;
- Nozzle size;
- Stand off distance;
- Mixing tube diameter;
- Forward angle;

During the experimental work only the cutting velocity and plate thickness are changed, leaving for the Future Work chapter some considerations to improve the analysis made.

2.4. Cutting Speed

According to Hashish, M. (2011), Fig 2.4-1 a) and b) shows a phenomenon associated to the abrasive waterjet cutting industry. When jets cut through and separate the material, several phenomena are observed. The first is that the jet is deflected opposite to the direction of the motion, phenomenon observed also by Valicek, J. *et al.* (2007). This means that the exit of the jet from the material lags behind the point at the top of the material where the jet enters. The distance by which the exit lags the entrance is called the trailback as shown in Fig 2.4-1 a). The second phenomenon is that the width of the cut varies along the cut from top to bottom, see Fig 2.4-1 b). This difference in width is designated the taper of the cut. A kerf taper can be either positive or negative, i.e. the width at the exit of the cut may either be smaller or larger than the width at the top. According to

Gudimetla, P. *et al.* (2002), the entrance width is inversely proportional to the cutting speed.
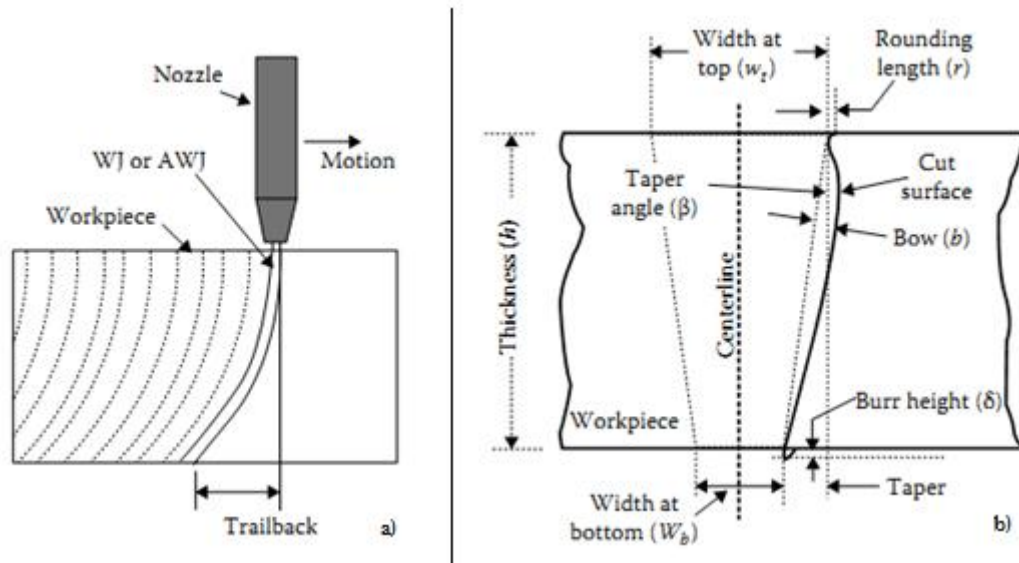
Fig 2.4-1 – AWJ cut attributes.

Chen, F. L. *et al.* (2003), described the surface waviness as a phenomenon related to AWJ cutting, see Fig 2.5-1, which is the macro level surface finish of the cut. The upper surface of the cut is free from waviness but still rough due to the abrasive erosion process (micro level material removal).

The waviness hypothesis is that the jet/material interface is not steady. During cutting a step of material moves under the jet until it reaches the bottom of the work piece, by Wang, J. and Wong, W. C. K. (1999). During this time, the jet traverses the plate and its effective diameter is reduced as it penetrates deeper.

Cutting speed has a major influence on kerf taper angle not only in metal, but also in composites, according to Shanmugan, D. K. and Masood, S. H. (2009).

2.5. Kerf Geometry

Another point of interest, explored during the dissertation is the kerf geometry. Fig 2.5-1 and Fig 2.5-2 shows a cut generated by abrasive water jets, aspect presented on Oliveira Santos, J.F. et al. (1991). It may be characterized by a small rounded corner at the top edge due to the plastic deformation of material caused by jet bombardment, as described by Hascalik, A. *et al.* (2007). As the kerf is wider at the top than at the bottom due to the decrease in water pressure, a taper is produced. In addition, the plastically

deformed material rolls over at the bottom of the kerf forming burrs at the jet. Two types of burrs were observed, hard burrs and loose hair line burrs.
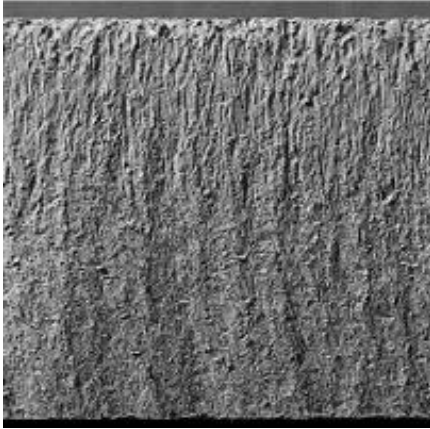
Fig 2.5-1 - Surface morphology produced by AWJ
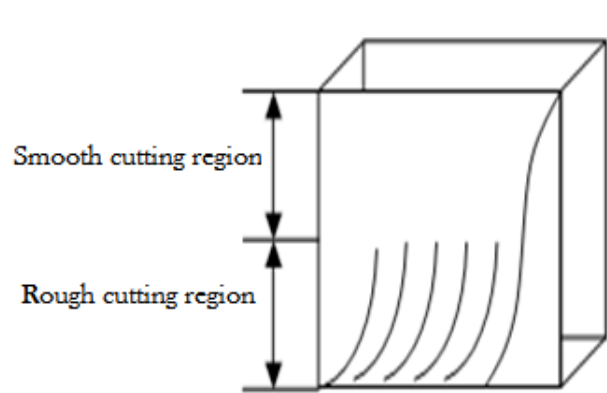
Fig 2.5-2 - Kerf geometry image example

Probably the most important aspect in kerf geometry is the taper angle, see Fig 2.5-3. According to Shanmugam, D. K. (2008), kerf taper angle is an undesirable geometrical feature inherent to abrasive waterjet machining.
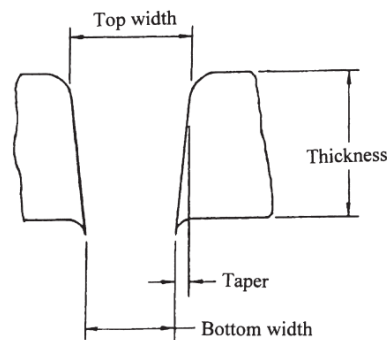
Fig 2.5-3 - Kerf width and kerf taper illustration

The majority of the taper angle measurement, found during the research is made by using a magnifying lens. The taper angle measurements will be done with a coordinate measurement machine.

3. Material, Equipment and Experimental Procedure

3.1. Material

The material studied was a SS 1312 (Swedish Standard) carbon steel RSt 37-2 DIN 17100 in 3 thickness of 2 mm, 4 mm and 6 mm. The Table 3.1-1 shows the nominal chemical composition of the material, and was taken from the internet http://www.zaporizhstal.com.

Table 3.1-1 – Chemical composition of the steel

Steel grade	Standard	Fraction of total mass of elements, %				
		C	Mn	P	S	N
RSt 37-2	DIN 17100	≤ 0.17	≤ 1.4	≤ 0.045	≤ 0.045	≤ 0.009

The 4 mm and 6 mm plates presented a coating, possible to see on the Fig 3.1-1.
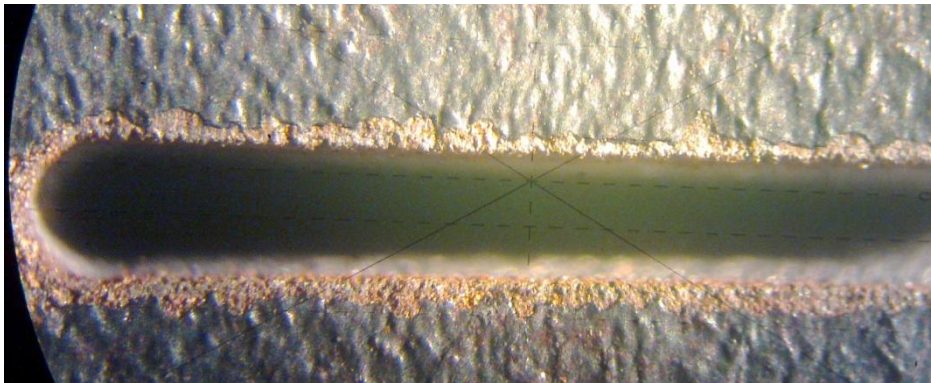
Fig 3.1-1 - Oxides present on the cutting surface from the 4 and 6 mm plates thickness

The coating is not mentioned during the tests, because it did not represent a problem for the waterjet cutting processes, as was proved in the article written by Wang, J. and Wong, W. C. K. (1999).

3.2. Waterjet Cutting

3.2.1.   Machine

The waterjet cutting machine in which the tests were made is an OMAX 5555 Jet Machining Center, see Fig 3.2-1. This model cuts complex flat parts out of most materials like metal, plastic, glass, ceramics, stone and composites, directly from a CAD drawing or DXF file. It is a standard model with the OMAX MAXJET® 5i Nozzle, and boasts a cutting tolerance of ±0.003"(±0.08 mm), retrieved information from the company website http//:www.omax.com. It comprises a completely sealed and protected Ball Screw Drive System, providing robustness and reliability, while offering high precision.

The main characteristics of the machine are indicated in Table 3.2-1.

Fig 3.2-1 - Water Jet Machine P5555

Table 3.2-1 –Characteristics of the OMAX 555 Jet Machining Center

Machine Dimensions	Footprint (with controller)	3,327 mm x 2,413 mm
	Weight (tank empty)	2,854 kg
	Height (with scissor pumbling)	2,998 mm
	Operating Weight (with water in tank)	5,987 kg
Work Envelop	X-Y travel	1,397 mm x 1,397 mm
	Table size	2,032 mm x 1,650 mm
	Material Supported Slats	101 mm x 3,175 mm
	Material Load	1,950 kg/sq meter
Accuracy of Motion at 20 ºC	At Max. Transverse Velocity	+/- 0.08 mm
	Repeatability	+/- 0.051 mm

	Squareness	0.17 mm/m
	Straightness	0.25 mm/m
	Backlash	0.018 mm
Speed	4,571 mm/min standard	
Noise Level	Below 80 dBA for submerged cutting	

3.3. Programming the Waterjet Machine

For programming the waterjet machine we either create the shape directly in one of the programs named LAYOUT or we export CAD drawings or DXF files to the same program.
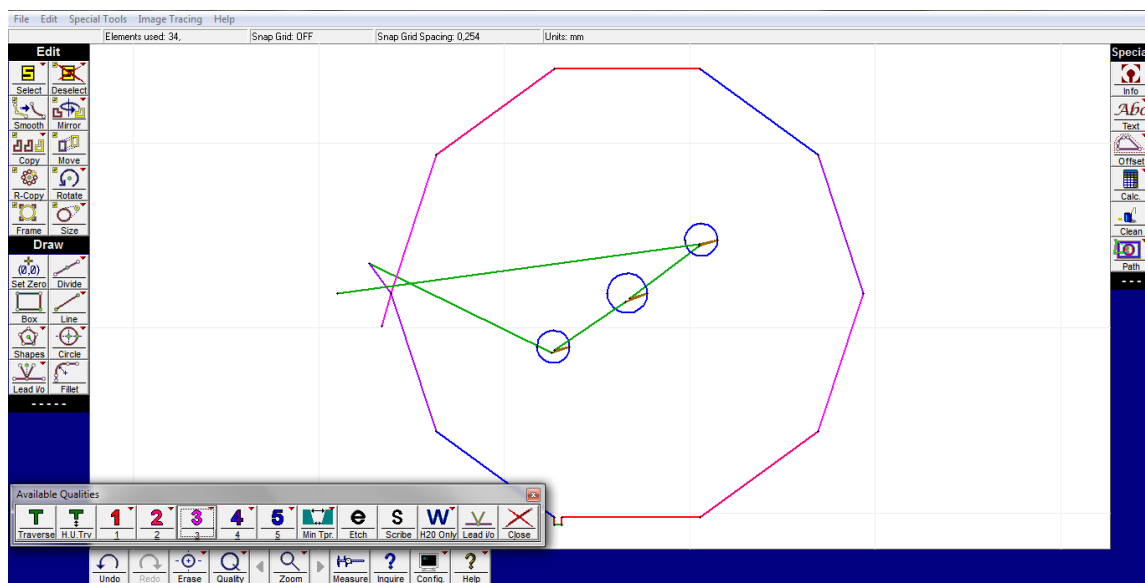
Fig 3.3-1 - LAYOUT program with Decagon design

In this step of the program we create the shape that we want to cut and select the quality that we want the surface to have. The LAYOUT program, Fig 3.3-1, has already pre-determined to which velocity correspond to which quality. Along with the surface quality we need to create guide lines marked with the green color. These lines connect all the elements; they give us the path that the nozzle will do during the cutting step, as illustrated in Fig 3.3-1.

After saving the document in the LAYOUT program, we press the path function, which provides a set of template paths or the ability to draw our own.

The next step will be opening the draw with the path defined in the MAKE program Fig 3.2-1. The MAKE program allows changing several items:

- Material you want to cut;

- Thickness;

- Tool offset;

- Rotation;

- Scale;

- Cutting settings;

- Pierce settings.
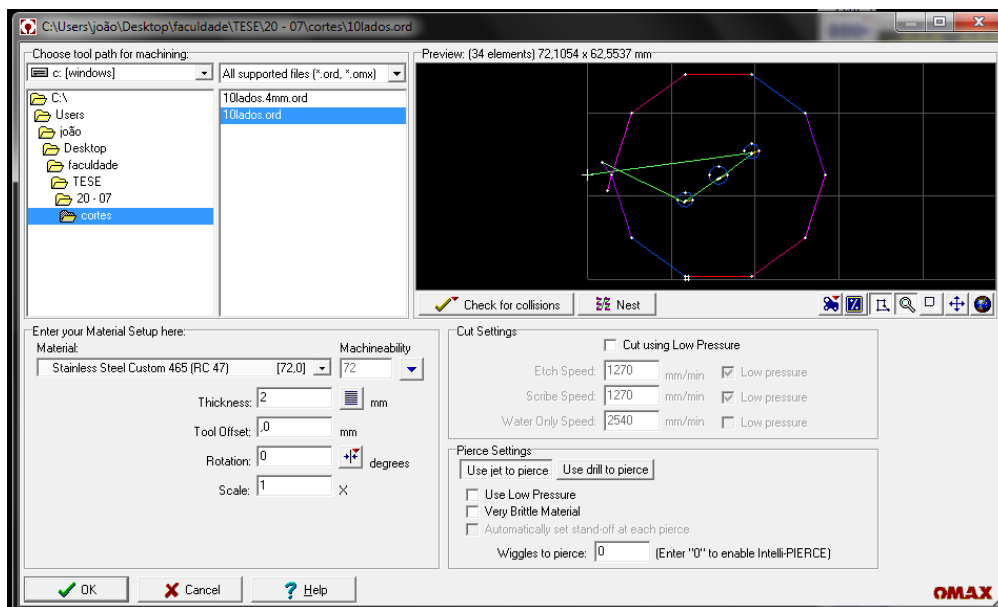
Fig 3.3-2 - MAKE program

One important aspect that needs to have some relevance is the tool offset. The Tool offset is the amount that is shifted away from the part to be cut. Tool Offset = 1/2 of the kerf width of the cutting nozzle. This compensates for the stream of abrasive water not being infinitely thin. For all test done in the work, the tool offset was equal to zero. When all the parameters are correct, we are now ready to position the nozzle at the right spot.

The first thing we need to do before defining our "home" is to calibrate the machine, so that the nozzle keeps within the table boundaries. The nozzle will move to the beginning of the X's and Y's axis.

The machine has a cutting angle of ±8º degrees, where 0º is the vertical rest position of the nozzle. Calibrating the nozzle is the next step. It is very important to secure the perpendicularity of the nozzle towards the table. By moving the arrows in the

keyboard, it is possible to position our "home" in the exact spot we want to start. The position of the nozzle in the Z's axis is influential on the final result. Positioning the nozzle too far away or too close from the work piece will not cut properly. The OMAX Company defines 0, 06 inches (1.54 mm) as the perfect stand-off distance.
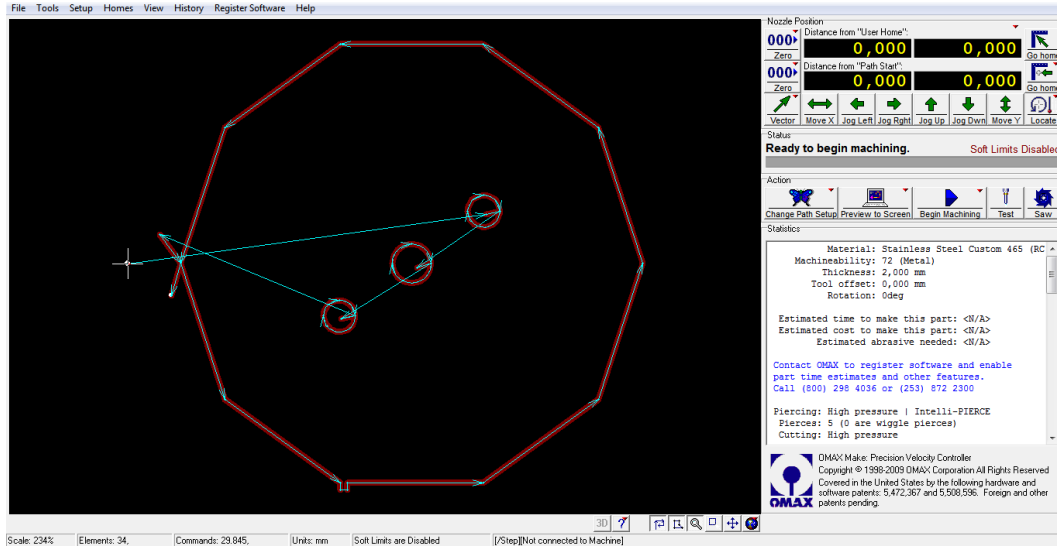
Fig 3.3-3 - MAKE program, final step

Sending the nozzle to the defined position in the Z axis, turning on the pump and floating the tank are the last step before pressing the start button. The last step on programming the waterjet machine is complete, as illustrated in Fig 3.3-3.

The OMAX MAKE program let us keep a word file of all parameters involved in the process, such as:

- All the ideal linear speed according to the quality;
- Estimate time to make the part;
- Estimate cost to make the part;
- Estimate abrasive needed;
- Total time spent cutting;
- Total time spent transversing;

The first parameter, all ideal linear speed according to the quality, will be the only one from the list, presented during this experimental work. The time and abrasive

spent in the piece cutting process provides a metric of one fundamental industry aspect, the time vs. money tradeoff.

This analysis must take into consideration the velocity, quality and thickness concepts. In this kind of machine it is not possible to change the velocity. The MAKE program only accepts the change of thicknesses. It incorporates all the equations needed to give the correct velocity for each thickness chosen. Increasing the thickness is slowing down the velocity. So in order to change the velocity I am forced to change the thickness, as illustrated on Fig 3.3-2.

I will have three real plate thicknesses (2, 4 and 6 mm) but for the program real and virtual thicknesses have been defined (1, 2, 3, 4, 5, 6 and 7 mm), in order to assess the cutting speed influence.

3.4. Abrasive

In this work, BARTON Company abrasive has been provided, Fig 2.4-1.

The abrasive type is the garnet 80 mesh HPX (150 to 300 μm). This abrasive provides great versatility for a wide variety of applications. It offers fast cutting speed and good edge quality, and is able to cut through a variety of different materials, including all metals, composites, ceramics and stone, as stated in http://www.barton.com. This garnet is formed by 97-98% of Almandine and 2-3% of Ilmenite, Quartz & Other. The Almandine chemical Composition is $Fe_3AI_2(SiO_4)_3$.

From the website http://www.minerals.net, Almandine is the most common form of the gemstone garnet. The term garnet describes a group name for several closely related minerals that form important gemstones, and Almandine is an individual mineral member of the garnet group. Almandine is usually opaque and unfit for gemstones use.

Fig 3.4-1 - Abrasive Bag

Fig 3.4-2 - Abrasive morphology

The HPX grains can be described as sharps angular crystals, see Fig 3.4-2. Because of these sharp and more angular edges, BARTON HPX is able to provide a fast cutting speed.

3.5. Coordinate Measuring Machine

The perpendicularity of cut faces is measured in terms of kerf taper angle, as illustrated in Fig 3.5-1, by a Coordinate Measuring Machine (CMM). The CMM available at the lab was a PMC V850 Zeiss west Germany with different stylus probe, see Fig 3.5-1. The smallest diameter probe (2 mm) was chosen and provides the stylus probe used in all the workpieces measurements. As the plate thicknesses are of 2 mm, 4 mm and 6 mm, it would not be wise to measuring it without the same stylus probe.

The main characteristics of the PMC machine, retrieved from http://www.zeiss.com/, are the following:

- Ultra high precision with an extremely low measuring uncertainty;
- Used for maximum precision measurements in research, development and quality assurance, as well as for the calibration of gages and test pieces;
- CNC-controlled, high-precision measuring machine with bridge-type central drive for acceleration-free measuring and constant precision throughout the measuring range;
- Fine Computer Aided Analyzes (CAA) for guide way error correction and position-dependent bending correction of the machine rigidity;
- Table plate bending compensation;
- Ultra High Precision Coordinate Measuring Machine (UPMC) offers ZEISS active scanning to capture very large quantities of data, graphic user guidance and efficient interfaces between the operator and measuring machine, simultaneous determination of size, form and position, and function-oriented inspection with a ring gage or mandrel.

Fig 3.5-1 - Coordinate Measuring Machine

This CMM operates with CALYPSO 5.0 software. For the angle results, it is possible to have two different ways for programming. Both serve the same purpose, create a plane. The two different ways for creating a plate are:

1. Define few points of the surface (without Polyline), typically 5 points;
2. Create a Polyline on the surface, typically 90 points. A Polyline is created by taking few points of the surface; these points will create a line which the program will use to scan the surface. During the scan, the program will take multiple points.

A plane with a high number of points provides better results. With only a few points the deviation of the plane angle is much bigger. The plane created by the Polyline is an accurate approximation. Marking those points may pose a problem. Since the navigation of the controllers and the needle's position is manually operated, it is easy to introduce error to the measurements. It was particularly difficult to measure the 2 mm plate thick.

One other problem found during the angle analysis was the fact that along the 20 mm face wide the velocity of the jet is different. Due to a design geometry constraint, the cut velocity will be higher on the center of the surface than on the surface ends. To have the same velocity in the entire 20 mm cut surface, in the LAYOUT program, the design of the border lines should be prolonged, at least until the entire surface is covered by the same cutting velocity. This aspect has a major influence marking the points for the Polyline, in the way that the plane does not represent the entire surface.

Two techniques were used for comparing the angle results:

1. Polyline;

2. Without Polyline;

In the Appendix, the tests carried out for the former two options are presented, where it is clear the differences in results underlying each of the used techniques. The first technique presents the most reliable results. The latter technique is discarded, due to the number of points taken for each measurement that provides a cruder plane characterization. Therefore the Polyline technique was the chosen technique for the study carried out.

3.6. Surface Roughness Measuring Instrument (SRMI)

The machine used for measuring the surface roughness was a TalySurf 4 (TAYLOR HOBSON Company), see Fig 3.6-1.

Fig 3.6-1 - Roughness machine

Fig 3.6-2 - Ra value monitor

The measured output is the average roughness, R_a, see Fig 3.6-2. From the website http://www.preved.com, the average roughness is the area between the roughness profile and its mean line, or the integral of the absolute value of the roughness profile height over the evaluation length, given by equation 1.

$$R_a = \frac{1}{L} \int_0^l |r(x)| dx \qquad\qquad 1)$$

Ra = average roughness; L = evaluation length; r(x) = profile function

Graphically, the average roughness is the shaded area between the roughness profile and its center line divided by the evaluation length, as illustrated in Fig 3.6-3, (typically each measurement is computed from five samples taken from the cut length).
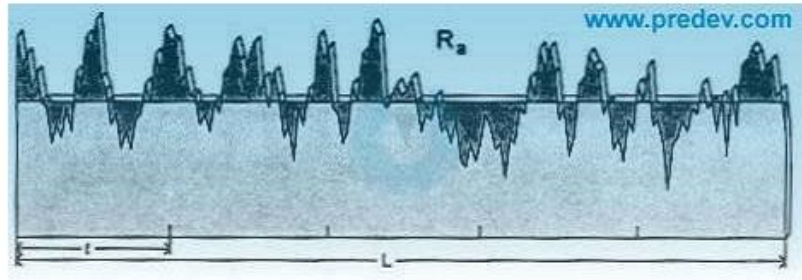
Fig 3.6-3 - Ra profile example

R_a is the most commonly used roughness parameter. However, the average roughness may provide, under a set of circumstances, the same value for set of different surfaces.
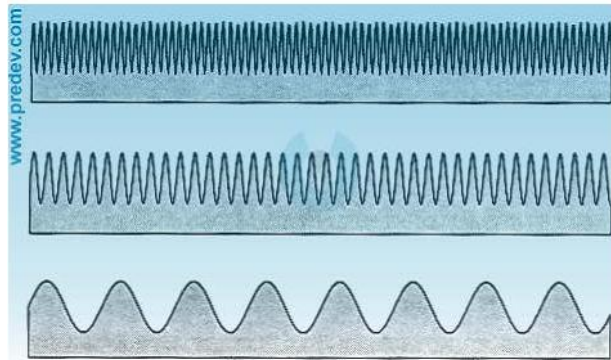
Fig 3.6-4 - Surface profile example

Despite having the same Ra value, Fig 3.6-4, shows three completely different surfaces. The R_a value alone, it is not the best solution to fully categorize the surface. R_q (Root Mean Square Roughness); R_t (total Roughness); R_y or R_{max} (Maximum Roughness Height Within a Sample Length); R_p (Peak Roughness); R_v (Depth of the Deepest Valley) are others parameters that can define the surface, although they have not been used.

For better analyzing the surface, this machine allow us to keep a graphic paper record from the cut surface roughness.

Fig 3.6-5 - Paper register machine

With this paper record it is possible to compare different cut surfaces, as demonstrated on Section D of the Appendix. The two paper samples are regarding to the test #1.6 and #3.6 – 6 mm plate thick.

3.7. Magnifying lens

The fourth machine utilized during the experimental work was a magnifying lens with live streaming connected to the computer. This connection allows analyzing in detail the cut surface. The objective is to scan the surface looking for any irregularity, as well as understand visually the surface difference cut with different cutting speed.

The analyses was divided in two categories, Surface Area and Kerf Geometry each one with its own objective and cut design. For the surface area, pictures of the surface regarding to quality 1 (faster velocity) and quality 5 (slowest velocity) were taken. As explained further, this analysis was made in the Decagon design. For the kerf geometry pictures from the cut surface were taken and the distances between each side of the cut were measured. The Comb design is the responsible for this analysis.

The magnifying lens had another advantages, allowing scanning the surface searching for abrasive or any other kind of particles embedded in the surfaces. When dealing with metal it is uncommon to find embedded abrasive particles. Since the cuts were made underwater, and the water was dried with a pressurized air gun, the abrasive was either washed away during the cut or during the cleaning processes.

3.8. Experimental Procedure

3.8.1.   Workpiece Geometry

One of the most important aspects of the whole experimental work is the correct design of the workpieces. It has a great importance because of its pivotal influence on this work basis. A correct choice must be made regarding the work direction. A tradeoff clearly exists between time, scientific interest and both scientific and experimental profit. In order to reach such a compromise, the two following geometries are proposed.

Geometry 1

The first geometry is a Decagon design, as illustrated in Fig 3.8-1. Fig 3.8-2, all the Decagon designs are shown. All the sides have the same length, 20 mm. The main reason to create this kind of design was to incorporate in the same workpiece the five available qualities on the LAYOUT program, replicated twice on the ten different faces, see Table 3.8-1 and Fig 3.8-1.

Table 3.8-1 – Face Vs. Quality

Faces	Quality
1 and 6	5
2 and 7	4
3 and 8	3
4 and 9	2
5 and 10	1

Having twice the area to analyze allowed discarding any deviation in the results, mainly created by jet deflection.

The three holes represented in the center of the plate with quality 5, were made for the purpose of holding it to the platform in the coordinate measuring machine.
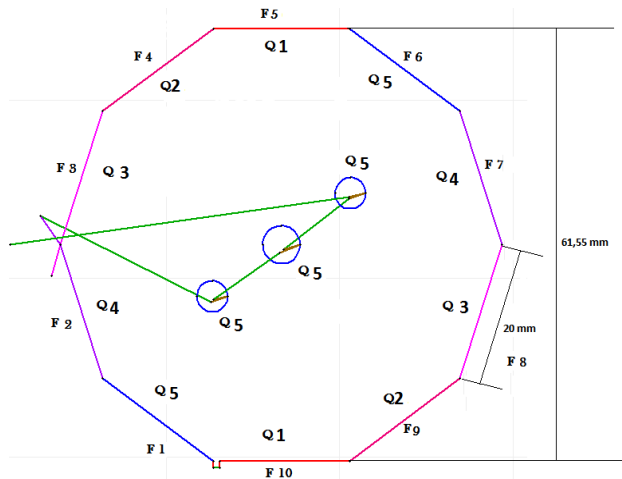
Fig 3.8-1 - Decagon geometry

Fig 3.8-2 - All Decagons work piece (2 mm, 4 mm and 6 mm)

For each quality Q_1 to Q_5 there is the correspondent face F_1 to F_{10}.

Table 3.8-1 – Face Vs. Quality

Faces	Quality
1 and 6	5
2 and 7	4
3 and 8	3
4 and 9	2
5 and 10	1

Faces 2 and 3 have more than 20 mm, as illustrated in Fig 3.8-1, and are the beginning and the end of the cut, respectively. Although it is a structural steel there is no risk when piercing the material, it is wise to start and end the cut outside the limits, problem found when cutting composites as described by Antunes, N. C. A. (2011), "Cutting of Carbon Fiber Reinforced Polymer Using Abrasive Water Jet Technology", Master thesis in Mechanical Engineering, University of Coimbra and by Wang, J. (1999). Fig 3.8-3 shows some important details of the Decagon design, like the position of the Tab, the direction of the cut and the beginning and ending of the cut.
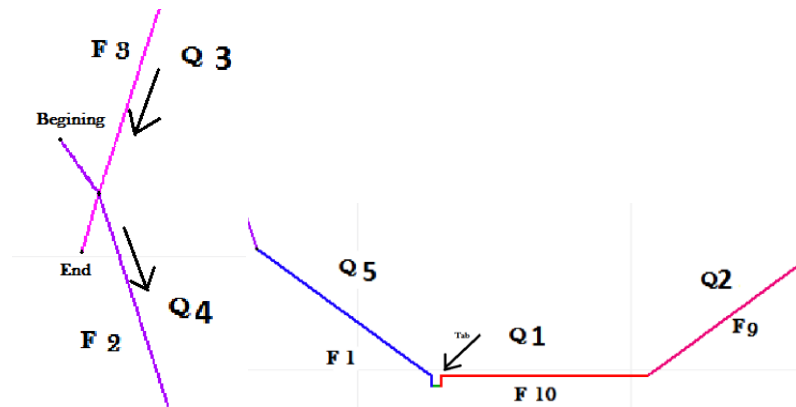
Fig 3.8-3 - Details of Decagon geometry

Geometry 2

The Decagon design presented in geometry 1, poses some constraints, as some characteristics are impossible to analyse with such geometry. Thus, a second geometry, designated Comb, was designed, see Fig 3.8-4. This new design allows to measure the distance between each cut side in top and bottom positions, while providing the ability to visualize the angle produced.
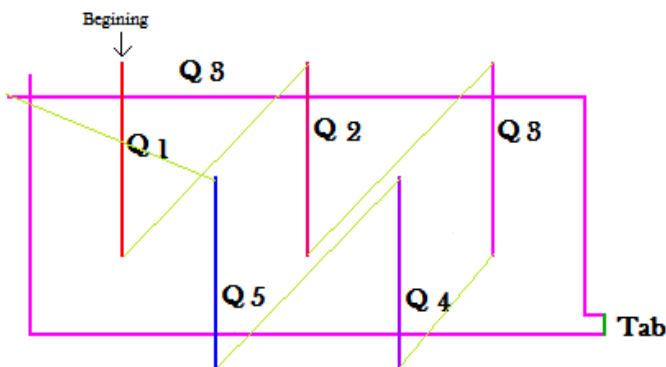
Fig 3.8-4 - Comb geometry

Fig 3.8-5 - All Comb workpiece (2 mm, 4 mm and 6 mm)

Fig 3.8-4 shows the Comb geometry; all the 5 qualities are presented. Fig 3.8-5 shows the Comb workpieces used in this dissertation. The jet came from outside the workpiece and started to cut 2 mm away from the border following the green guidelines. The outline border does not have any influence in this analysis.

Tab

On the Decagon design, between F_1 and F_{10}, a small square is noticeable, see Fig 3.8-3, and named Tab. It is a very important fixture, created by hand or with the possibility of using one already established by the program LAYOUT. The tab has the function of holding the workpiece we want to cut on the main plate, as shown in Fig 3.8-6. With this function there is no risk of seeing our cut piece drawn into the tank. This square has 1mm x 1mm (length x height) and is present in all workpieces.

On the Comb design, the tab function is equally present and with the same dimensions.
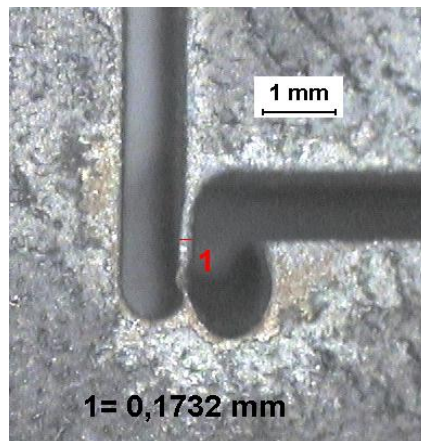
Fig 3.8-6 - Tab from the test #1.6

3.8.2. Procedure

The experimental work can be divided into two parts. The first part concerns to the Decagon workpiece geometry, and the second part is regarding the Comb workpiece geometry. The evaluations made in the Decagon geometry are:

1. The surface roughness, measured with a surface roughness measuring instrument (SMRI);
2. The kerf taper angle, measured with the CMM;
3. Surface Area, with magnifying lens.

The evaluation made in the Comb geometry is made by a magnifying lens to measure the distance between each cut side, on top and on bottom position.

For the entire tests made, the only parameter that was changed was the thickness. Parameters indicated in Table 3.8-2 were maintained constant during the entire tests.

Table 3.8-2 - Pressure and Nozzle Setup

High Pressure Settings	3447.38 [bar]	344.738 [Mpa]
Low pressure Settings	1378.95 [bar]	137.895 [Mpa]
Mixing Tube Diameter	0.762 [mm]	
Jewel Diameter	0.3302 [mm]	
Abrasive Flow Rate	0.35 [Kg/min]	
Abrasive Index	1	

The objective of this dissertation is to analyze the influence of the cutting speed in carbon steel plates. The OMAX program is very restrict on the function available for cutting, the only way to change the velocity is by changing the thickness, as referenced before. Therefore on the 2 mm, 4 mm and 6 mm plate thickness several workpieces have different defined thicknesses, or virtual thicknesses, in order to vary the jet velocity. Namely, the following virtual thicknesses were defined for the plate thicknesses below:

2mm plate:

- One specimen cut as if it was 1 mm thick;
- One specimen cut with the real thickness, 2 mm (in this case, the virtual thickness matches the plate thickness);
- One specimen cut as if it was 3 mm thick.

4 mm plate:

- One specimen cut as if it was 3 mm thick:
- One specimen cut with the real thickness, 4 mm (in this case, the virtual thickness matches the plate thickness);
- One specimen cut as if it was 5 mm thick;
- One specimen cut as if it was 6 mm thick.

6 mm plate:

- One specimen cut as if it was 5 mm thick;
- One specimen cut with the real thickness, 6 mm (in this case, the virtual thickness matches the plate thickness);

- One specimen cut as if it was 7 mm thick.

The Table 3.8-3 resumes the test made and the differences in the thickness as well as the code name presented for each test.

Table 3.8-3 - Test code

Thickness	Test Number [#] – Meaning
2 mm	#1.2 – virtual thickness – 1 mm #2.2 - real thickness – 2 mm #3.2 - virtual thickness – 3 mm
4 mm	#1.4 - virtual thickness – 3 mm #2.4 - real thickness – 4 mm #3.4 - virtual thickness – 5 mm #4.4 - virtual thickness – 6 mm
6 mm	#1.6 - virtual thickness – 5 mm #2.6 – real thickness – 6 mm #3.6 - virtual thickness – 7 mm

The procedure for Comb geometry is totally similar to the Decagon geometry. All pieces are equally marked and have the same orientation, face matching quality and tab position.

4. Presentation and Results Discussion

In this chapter, results from each cut will be presented regrouping them by plate thickness; there will be also a comparison between workpieces cut with the same cutting velocity but with different thicknesses, as shown in Table 3.8-3.

The results presentation will follow some guidelines. Firstly, the results will be presented according to a plate thickness ascending order, first from the Decagon and then from the Comb design. Results from AWJ, SRMI, CMM and magnifying lens, are then presented. Also some references to the amount of burr formed during the cut process are mentioned.

4.1. 2 mm plate thick

As discussed by Wang, J. and Wong, W. C. K. (2008), the possibility of bending the plate was a concern. If that occurs it would be catastrophic in the final geometry and it could be dangerous, because it could hit the nozzle destroying it or even deflecting the water jet creating some serious damages. However, bending was not reported on any of the 2mm plate thickness workpieces.

According to Table 3.8-3, the 2 mm plate thick has three scheduled tests, programmed assuming 1, 2 and 3mm thickness, giving the following relations:

- #2.2 (2mm) to #1.2 (1 mm) → increase of +52 % in the velocity
- #2.2 (2mm) to #3.2 (3 mm) → decrease of -25 % in the velocity

Table 4.1-1, shows the proportion values between the three tests.

Table 4.1-1 – 2 mm plate thick. Velocity values according AWJ system

Test#	Velocity [mm/min]		
Quality	#1.2	#2.2	#3.2
1	1483,23	978,01	724,34
2	1272,09	838,01	621,23
3	798,02	526,2	398,71
4	573,23	377,98	279,94
5	443,49	292,43	216,58

The velocity relation between all tests is the same during the three tests.

4.1.1. Roughness Test

Using the SRMI described earlier, each surface was measured in the same conditions twice. Especially in this thin material, is very difficult to place the needle exactly on the top or in the bottom of the surface. The measurement of the Ra values was very difficult because the surface is not always free from burr (aspect found mainly in the 2 mm plate thick). Some results were discarded as they were identified to be outliers. The increased surface area due to two faces per cutting speed, allowed investigating those Ra outlier values.

Table 4.1-2, Table 4.1-3 and Table 4.1-4 shows the average roughness values measured in the SRMI. The measurements were made on top, middle and bottom position, being the top position the closer to the entry point.

Table 4.1-2 - Ra values for test #1.2 mm thick

#1.2 [µm]			
Position Quality	Top	Middle	Bottom
1	7,8	7,4	>10
2	7	9,4	>10
3	5,5	7	10
4	5,2	6	7,2
5	5	5	5,8

Table 4.1-3 - Ra values for test #2.2 mm thick

#2.2 [µm]			
Position Quality	Top	Middl	Bottom
1	7,8	8,2	>10
2	7,5	8	>10
3	5	5,8	6
4	4,2	4,8	6,5
5	4,9	4,2	4,4

Table 4.1-4 - Ra values for test #3.2 mm thick

#3.2 [µm]			
Position Quality	Top	Middle	Bottom
1	5,8	6	7,8
2	6	5,5	6,8
3	5,2	5	5
4	4,5	5	4,8
5	4	3,8	4,5

Some values went outside the monitor area, resulting in over 10 μm. In general the R_a value tends to increase with the depth of the cut thickness. Comparing the three tests, increasing the thickness (which means decreasing the velocity), the R_a value decreases, result expected according Wang, J. and Wong, W. C. K. (1999), Hascalik, A. *et al.* (2007) and by Akkurt, A. *et al.* (2004). However, in the measured results, some R_a values do not follow this relation, due to difficulties in positioning the needle in the required spot.

In order to compare the roughness of surface cuts of the three tests, the evolution of roughness as a function of the cutting speed is show in Fig 4.1-1, Fig 4.1-2 and Fig 4.1-3 respectively for top, middle and bottom of cut surface.
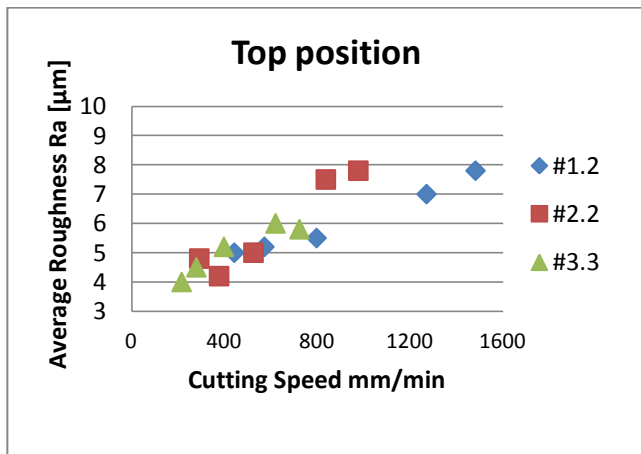
Fig 4.1-1 - Roughness Value Vs. Cutting speed on Top position. 2 mm plate thickness
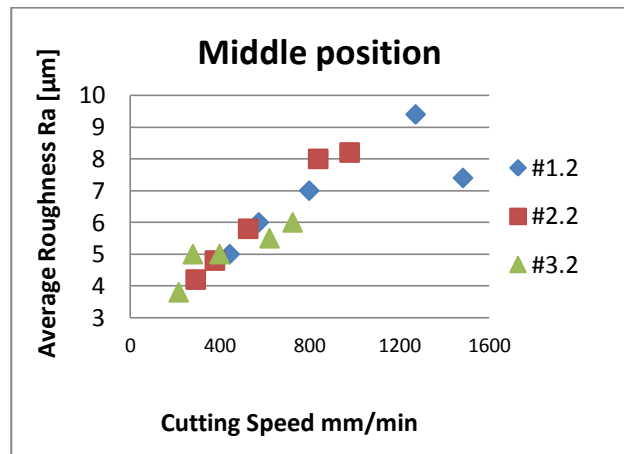
Fig 4.1-2 - Roughness Value vs. Cutting speed on Middle position. 2 mm plate thickness
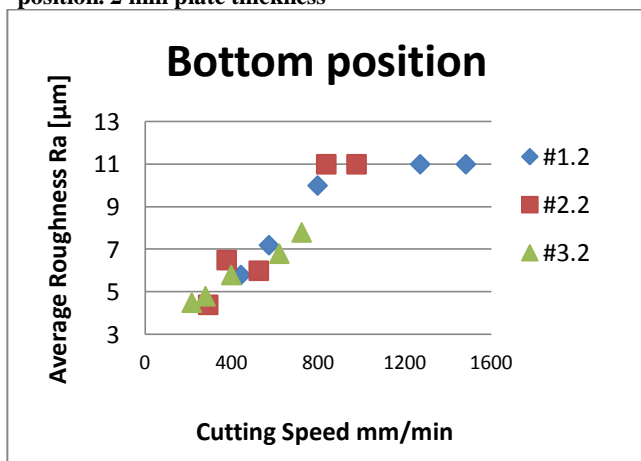
Fig 4.1-3 - Roughness Value vs. Cutting speed on Bottom position. 2 mm plate thickness

All the three Figures, Fig 4.1-1, Fig 4.1-2 and Fig 4.1-3, share the same kind of result. The slower the cutting velocity, the better the surface with look like as the R_a value

decreases. One other conclusion is the fact that the first test #1.2 (blue color) presents a higher R_a value than the third test, #3.2 (green color). The higher the virtual thickness the better the surface will be. The amplitude variation of the third test (#3.2) is very consistent for the three positions.

4.1.2. Kerf Taper

As described, the CMM was used to calculate the kerf taper angle from all the 10 faces presented on the Decagon design.

The 2 mm thickness was a barrier for collecting all the points in terms of using bare eyes to place the CMM stylus on the correct position. Since it is a 2 mm thick it was very difficult to reach all faces for colleting all the points in an efficient way. Therefore I have only examined 5 faces, as shown in Table 4.1-5 correspondent to the 5 qualities, suitable of presenting good results.

<p align="center">Table 4.1-5 –Face vs. Quality for the 2 mm plate thick</p>

Face	Quality
1	5
7	4
8	3
9	2
10	1

The Fig 4.1-4 refers to the Polyline strategy. In Section A of the Appendix, a comparison between the "Polyline" and the "Without Polyline" strategy is presented.
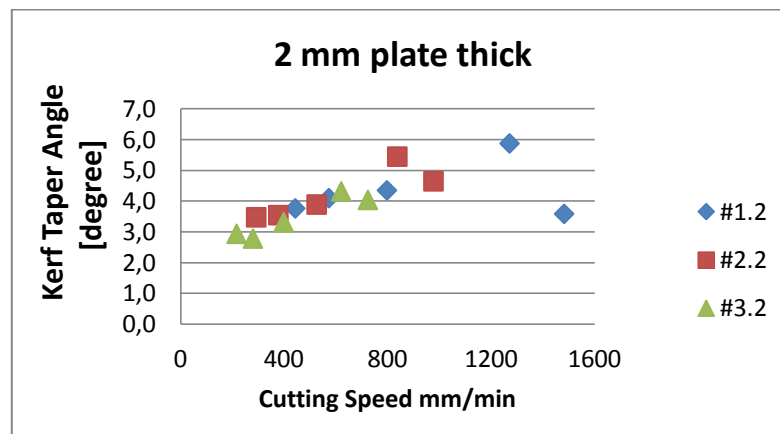
<p align="center">Fig 4.1-4 - Kerf taper angle Vs. Cutting speed. 2 mm plate thickness</p>

An interesting result is the fact that the taper angle value increases with the increase of the cutting speed until a certain velocity. Beyond such threshold, the taper angles start to decrease. The third test (#3.2) presents the lowest angle and the first test (#1.2) the highest. The higher the virtual thickness, hence the lower the velocity, the lower the taper angle will be. All the three tests have a similar graphic curve.

4.1.3.   Surface area

Scanning the surface, the entry and exiting points could represent the detection of new results. The red lines symbolize the trailback produced by the jet.

- First test #1.2, "virtual" thickness – 1mm thick
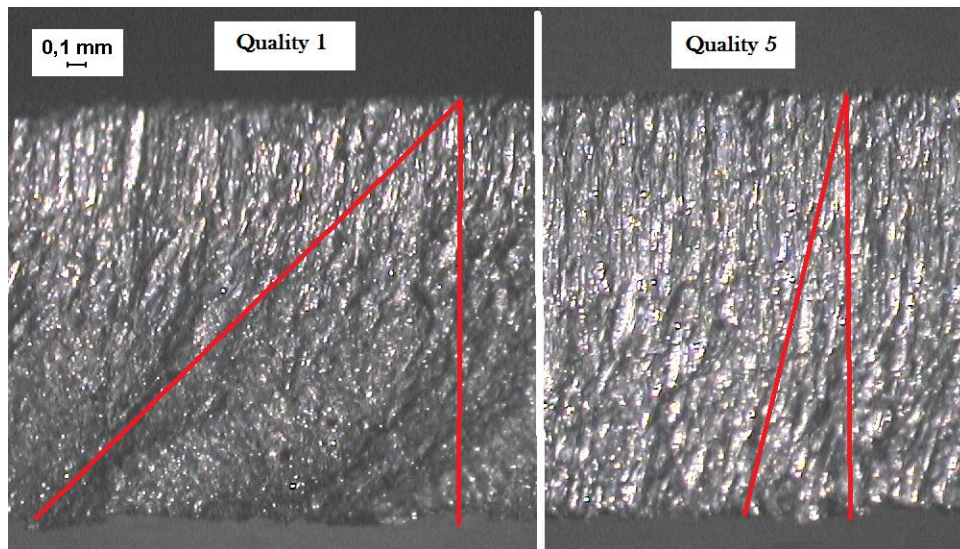
Fig 4.1-5 - Test #1.2. Quality 1 (1483.23 mm/min) Vs. Quality 5 (443.49 mm/min)

As the Fig 4.1-5 shows, there is a huge difference in the trailback. As it is possible to see, on the quality 1 (1483, 23 mm/min) the distance between the entry and exiting point presents higher distance then the trailback found on the quality 5 (443, 49 mm/min).

- Second test #2.2, real thickness – 2mm thick
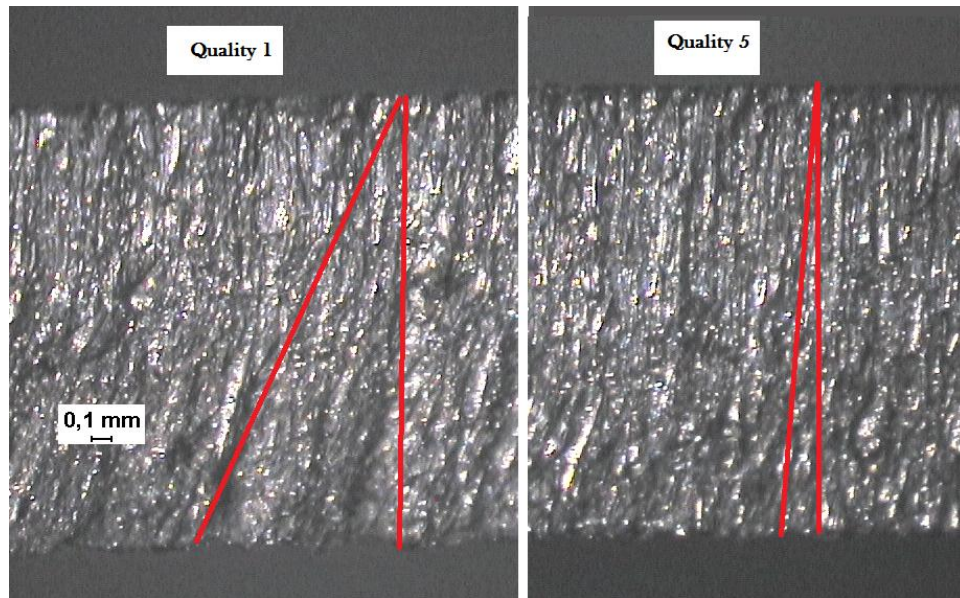
Fig 4.1-6 - Test #2.2. Quality 1 /978.01 mm/min) Vs. Quality 5 (292.43 mm/min)

Fig 4.1-6 shows the cut surface for test #2.2 (2 mm thick). The trailback in quality 1 (978, 01 mm/min) and quality 5 (292, 43 mm/min) is smaller when the one compare to the Fig 4.1-5.

- Third test #3.2, "virtual" thickness – 3mm thick
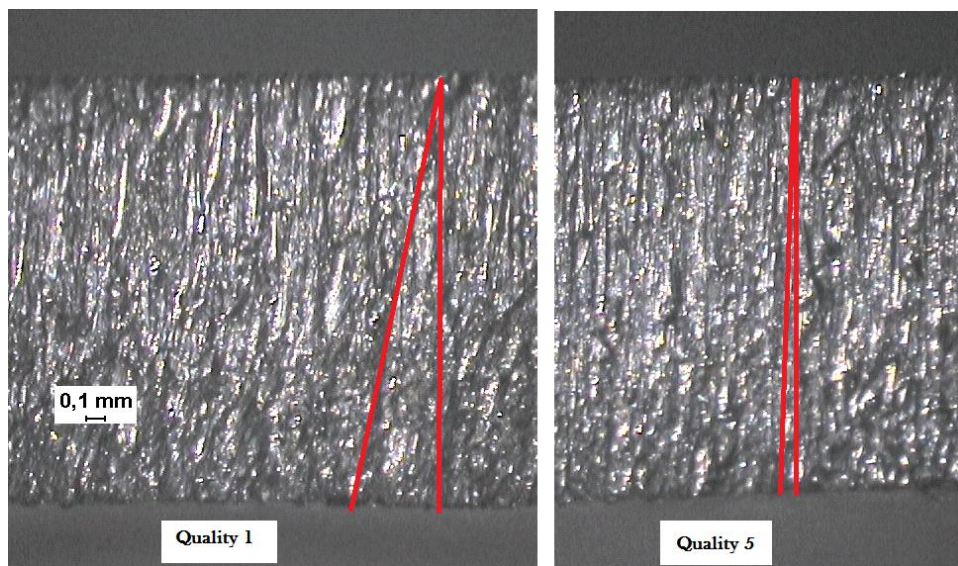
Fig 4.1-7 - Test #3.2. Quality 1 (724.34 mm/min) vs. Quality 5 (216.58 mm/min)

Fig 4.1-7 represents the third test made. Quality 1 (724, 34 mm/min) and quality 5 (216, 58 mm/min), are the lowest cutting velocity values for the 2 mm plate thick. It is notorious the approximation in the trailback distance for quality 1 and quality 5.

There is a visible difference on the surface between the quality 1 and quality 5 in all the tests carried out. The most noticeable is the #1.2, where those differences are completely clear, it is observable the waviness made by the jet and is very interesting to see the distance on the entry and the exiting point of the jet. The trailback distance decreases when the velocity is decreased.

4.1.4.   Kerf Geometry

Kerf geometry, has said previously, is measured on top and bottom positions. For the top analysis the measurements did not start at the very beginning of the plate because of the round corners produced by the jet impact, according to Wang, J. and Wong, W. C. K. (1999). For the bottom analyzes the measurement were made on the bottom of the workpiece.

Fig 4.1-8 shows that distance comparing the three tests made.
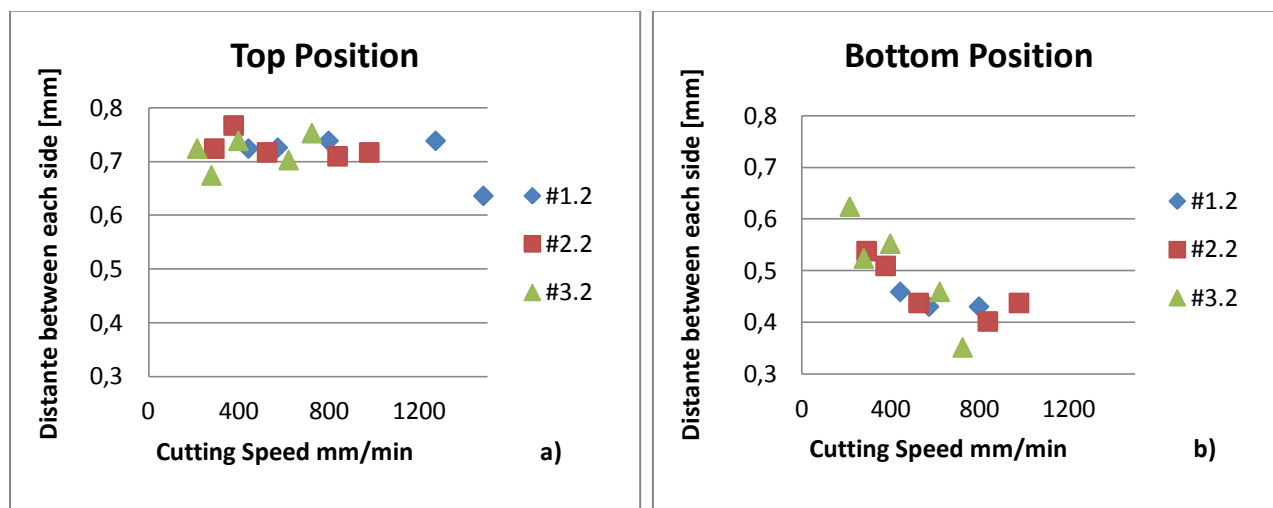
Fig 4.1-8 - Distance between each side of the cut. a) Top position; b) Bottom position

The graphic regarding to the Top position, Fig 4.1-8 a), has a lot of inconsistent results, probably due to any kind of error measuring it. The graphic showing the Bottom position, Fig 4.1-8 b), is more suitable for analysis. In a general way, the decrease in velocity results in an increase in the distance between each side, aspect substantiated by Oliveira Santos, J. F. (1991). For the first test #1.2, it only started at the quality 3 (798.02 mm/min) because it did not cut entirely in the quality 1 (1483.23 mm/min) and in quality 2 (1272.09 mm/min) as seen in Fig 4.1-9 and Fig 4.1-10.

The green points corresponding to the third test, presents the major distance than the other two. It is known that the decrease of the traverse speed produces larger distances on top and on bottom. By slowing the cut velocity, the beam stays longer in the same spot, having more time to cut through it. This effect produces two results, smallest taper angle and larger distances between faces, result obtain by Oliveira Santos, J. F. *et al.* (1991) and by Shanmgam, D. K. *et al.* (2008).
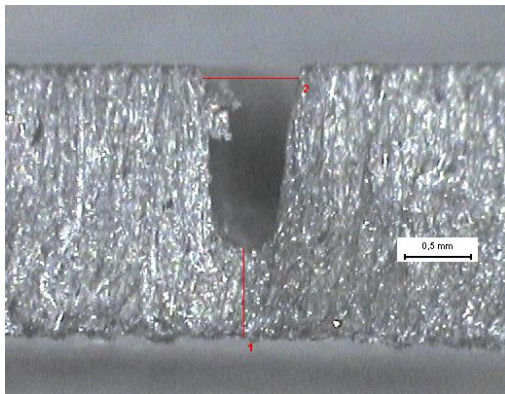
Fig 4.1-9 - Test #1.2. Quality 1 (1483.23 mm/min)
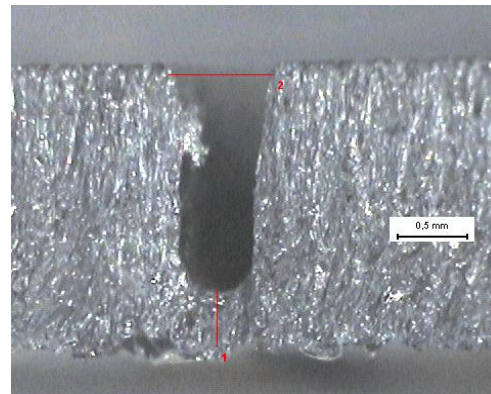
Fig 4.1-10 - Test #1.2. Quality 2 (1272.09 mm/min)

4.1.5. Burr

According to Wang, J. and Wong, W. C. K. (1999), the most interesting burr formation, is the hard burrs. As said earlier, the phenomenon behind hard burr formation is the plastic deformation. Hard burrs were found at the jet exit side where the material attached firmly around the bottom cut edges. This burr phenomenon occurs in every work piece, but is much more perceptible in the 2 mm plate thick. The burr height steadily decreases with the decrease in the cutting velocity. This is because slower velocities allow more thorough cutting and lower burrs to be formed. Increasing the standoff distance resulted in an increase in the burr height. This may be attributed to the jet power reduction as it flows away from the nozzle, resulting in high burrs due to the material deformation and roll over at low water pressure. For perfect surface finishing a secondary process is required.

4.2. 4 mm plate thick

According to Table 3.8-3, the 4 mm plate thick has four scheduled tests, programmed assuming 3 mm, 4 mm, 5 mm and 6 mm thickness, giving the following relations:

- #2.4 (4mm) to #1.4 (3 mm) → increase of +27 % in the velocity

- #2.4(4mm) to #3.4 (5 mm) → decrease of -18 % in the velocity

- #2.4 (4mm) to #4.4 (6mm) → decrease of -23 % in the velocity

- #3.4 (5mm) to #4.4 (6mm) → decrease of -6 % in the velocity

Table 4.2-1 shows the velocity relation between the four tests.

Table 4.2-1 - 4 mm plate velocity characteristics

Test# Quality	Velocity [mm/min]			
	#1.4	#2.4	#3.4	#4.4
1	724,34	570,69	467,52	441,08
2	621,23	489,46	400,97	378,3
3	389,71	307,05	251,54	237,32
4	279,94	220,56	180,68	170,47
5	216,58	170,64	139,79	131,89

The velocity relation between all tests is the same during the four tests.

4.2.1. Roughness Test

Table 4.2-2, Table 4.2-3, Table 4.2-4 and Table 4.2-5 shows the average roughness values measured in the SRMI. The measurements were made on the top, middle and bottom surface, being the top position the closer to the entry point.

Table 4.2-2- Ra values for test #1.4 mm thick

Position Quality	#1.4 [µm]		
	Top	Middle	Bottom
1	5,5	7,2	>10
2	4,6	6,8	7,2
3	3,8	4,8	5,5
4	3,8	4	5
5	4	4,2	5,5

Table 4.2-3 - Ra values for test #2.4 mm thick

Position Quality	#2.4 [µm]		
	Top	Middle	Bottom
1	4,8	6	8
2	4,6	5	6,5
3	4,5	5,2	4,8
4	3,8	4,8	4,8
5	3,8	4,5	4,5

Table 4.2-4 - Ra values for test #3.4 mm thick   **Table 4.2-5 - Ra values for test #4.4 mm thick**

#3.4 [µm]			
Position / Quality	Top	Middle	Bottom
1	4	5,5	6,2
2	4	5,5	5,5
3	3,8	,5	4,8
4	3,5	4,5	5
5	3,2	4,1	4

#4.4 [µm]			
Position / Quality	Top	Middle	Bottom
1	4	5	5,5
2	3,8	6	5,2
3	3,6	5	,5
4	3,2	4	4,8
5	4	3,6	4

Same results as the 2 mm plate thick were given for the 4 mm plate thick. Despite a few outliner results, the cut depth produces a increase in the Ra values. The roughness is improved by increasing the virtual thickness and decreasing cutting speed.

In order to compare the roughness of surface cuts of the four tests the evolution of roughness as function of the cutting speed is show in Fig 4.2-1, Fig 4.2-2 and Fig 4.2-3.
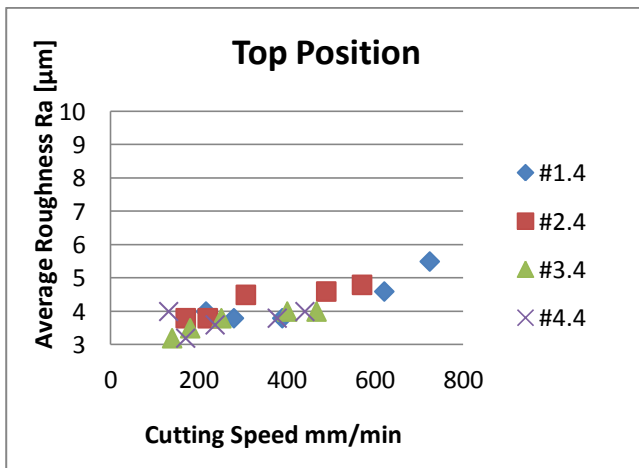
Fig 4.2-1 - Roughness Value Vs. Cutting speed on Top position. 4 mm plate thickness
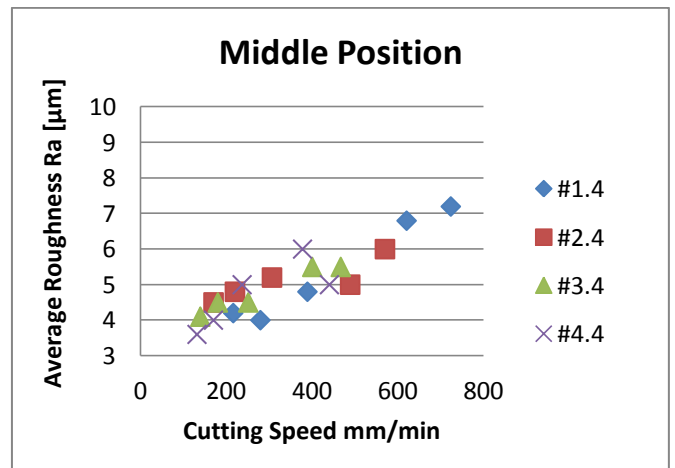
Fig 4.2-2 - Roughness Value Vs. Cutting speed on Middle position. 4 mm plate thickness
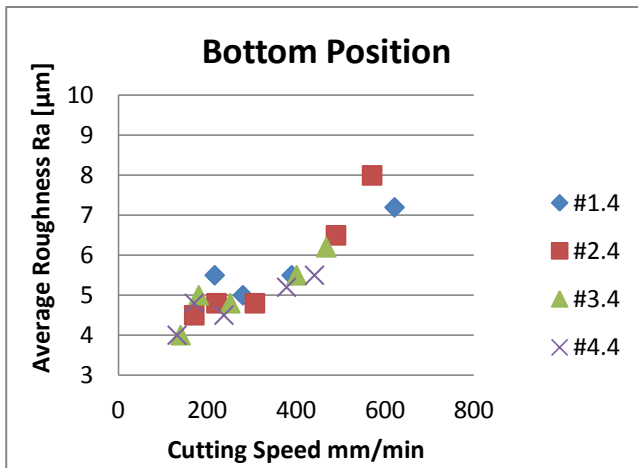
**Fig 4.2-3 - Roughness Value Vs. Cutting speed on Bottom
position. 4 mm plate thickness**

Following the same results as the 2 mm plate thick, the 4 mm plate thick in terms of comparing the roughness with the position is basically the same. Roughness is increased with the increase of cut depth, starting from the entry point. As concluded before the cut with the slowest velocity #4.4, presents better surface roughness, being the test #1.4, the faster which presents the worst surface.

4.2.2.   Kerf Taper

Having twice the thickness, allowed avoiding some barriers form the 2 mm plate thick. For the 4 mm thickness points from all the ten faces were taken. The reference (1-5) and (6-10) refers to which set of faces are being analyzed.

- (1-5) - faces 1,2,3,4 and 5
- (6-10) - faces 6,7,8,9 and 10

The Fig 4.2-4 and Fig 4.2-5 refers to the Polyline strategy. In Section B of the Appendix, there is the comparison between the "Polyline" and the "Without Polyline" strategy.
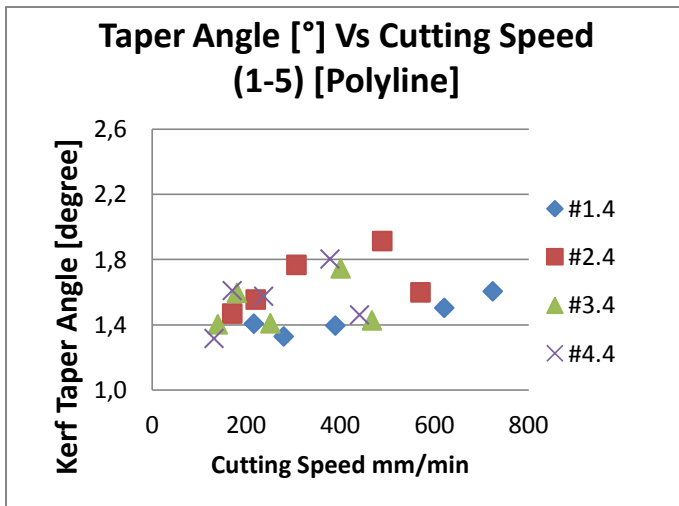
Fig 4.2-4 – Kerf Taper angle Vs. Cutting speed. 4 mm thick. Faces 1-5
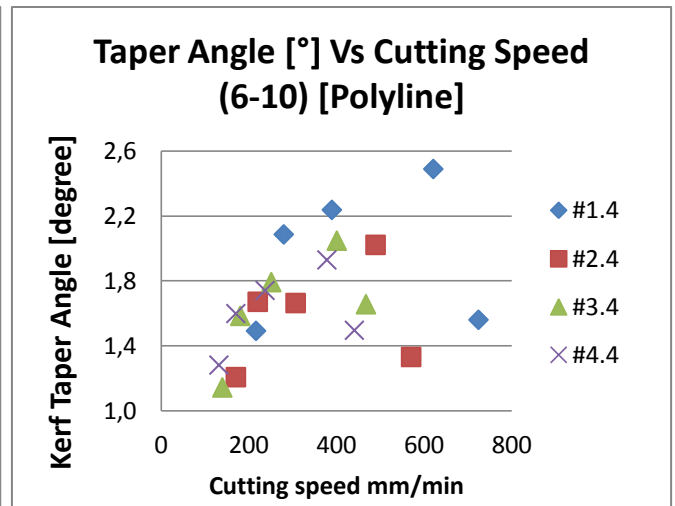
Fig 4.2-5 – Kerf Taper angle Vs. Cutting speed. 4 mm thick. Faces 6-10

There are some differences in the results regarding both set of faces. In Fig 4.2-4, the fourth tests #4.4, does not present the best angle, and the first tests #1.4, is not the worst, expected result taking into account the results from the 2 mm thick. Fig 4.2-5 shows a trend already analyzed. The taper angle is increased until a certain value, after that value the angle decreases. The amplitude variation is higher in the second graphic Fig 4.2-5. In a general approach, decreasing the cutting speed the angle tends to be smaller since the jet stays longer cutting.

4.2.3.   Surface area

4 mm plate will follow the guideline presented for the 2 mm plate. The red lines symbolize the trailback produced by the jet. In this 4 mm plate thick, as was possible to prove in Table 4.2-2, Table 4.2-3, Table 4.2-4 and Table 4.2-5 the R_a values are smaller than the values of the 2 mm plate thick.

- First test #1.4, "virtual" thickness – 3 mm thick (no image)
- Second test #2.4, real thickness – 4 mm thick (no image)
- Third test #3.4, "virtual" thickness – 5 mm thick
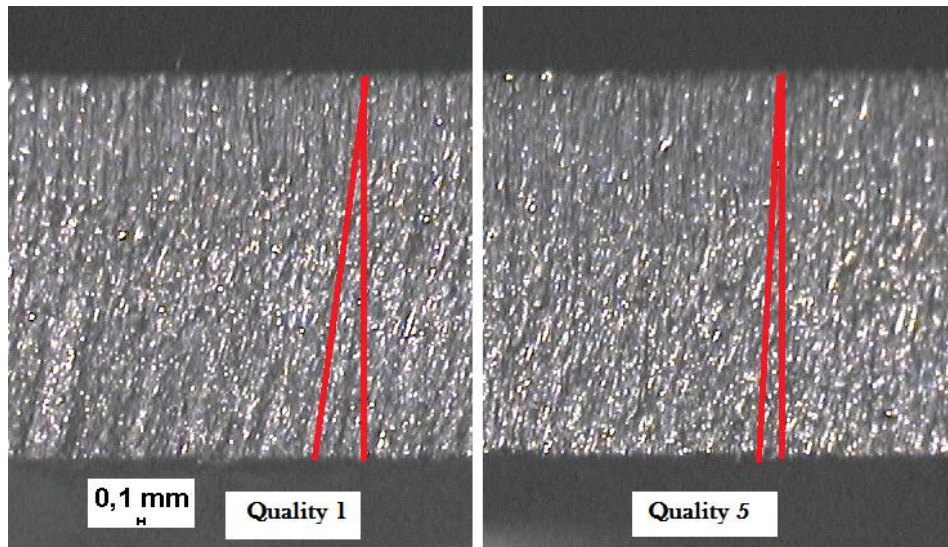
Fig 4.2-6 - Test #3.4. Quality 1 (467.52 mm/min) Vs. Quality 5 (139.79 mm/min)

The trailback presented in Fig 4.2-6 is an indicator of the good cut surface presented in this test. Either quality 1 (467, 52 mm/min) or quality 5 (139, 79 mm/min) presents smaller trailback distances.

- Fourth test #4.4, "virtual" thickness – 6mm thick
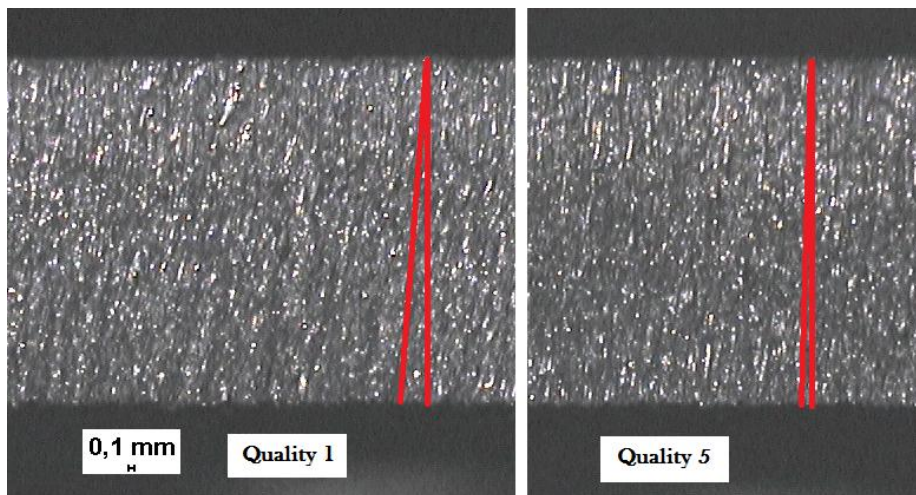
Fig 4.2-7 - Test #4.4. Quality 1 (441.08 mm/min) Vs. Quality 5 (131.89 mm/min)

Fig 4.2-7 shows how closely the quality 1 (441, 08 mm/min) and quality 5 (131, 89 mm/min) are in trailback distances.

Despite the analysis for the test #1.4 and #2.4 have not been made, form the results presented for the #3.4 and #4.4, is possible to say that decreasing the velocity is reducing the distance between entry and exiting point.

4.2.4.   Kerf Geometry

Top and bottom graphics are shown in Fig 4.2-8, comparing the distance between each side with the cutting speed for the four specimens.
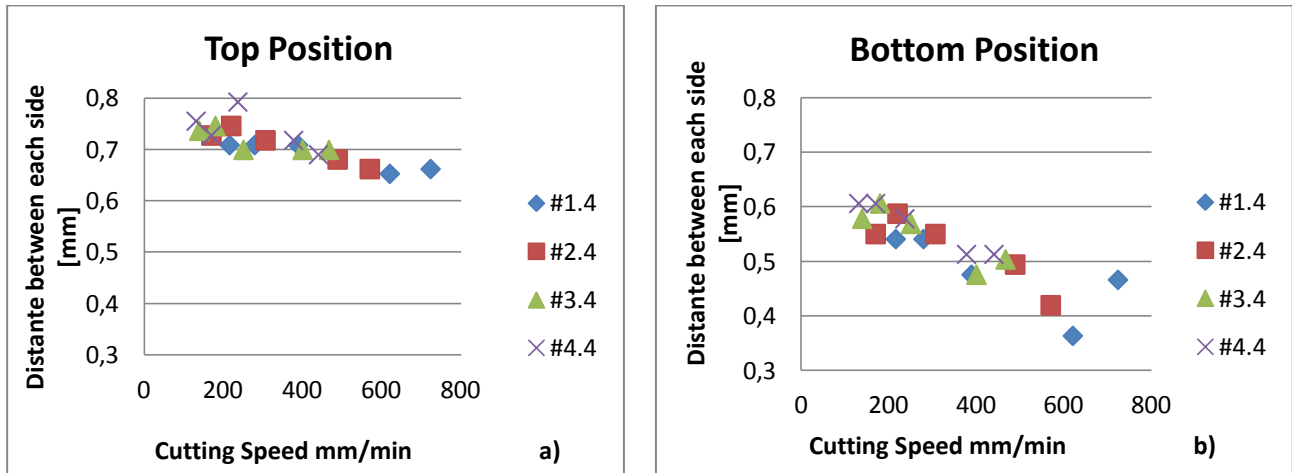
Fig 4.2-8 - Distance between each side of the cut. a) Top position; b) Bottom position

From the Fig 4.2-8 a) and b) is possible to conclude that increasing the cutting speed is decreasing the distance between sides. The test cut with the slowest velocity #4.4, presents the highest distance on top and bottom. The test #1.4, faster velocity, presents the smallest distances. The bottom position, see Fig 4.2-8 b), presents a familiar result, increasing the virtual thickness is increasing the distances between each side.

The Fig 4.2-9 allows us to understand more clearly this difference.
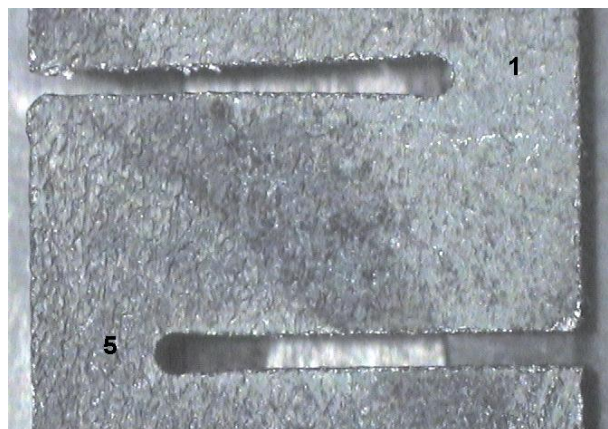
Fig 4.2-9 - Test #2.4. Quality 1 (570.7 mm/min) and quality 5 (170.6 mm/min), bottom comparison

This Fig 4.2-9, represent the back side of the Comb workpiece for the #2.4 test. Is visible the difference in the cut geometry, as was understood by Hascalik, A. *et al*. (2007).

4.3. 6 mm plate thick

According to Table 3.8-3, the 6 mm plate thick has three scheduled tests, programmed assuming 5 mm, 6 mm and 7 mm thickness, giving the following relations:

- #2.6 (6mm) to #1.6 (5 mm) → increase of +6 % in the velocity
- #2.6 (6mm) to #3.6 (7 mm) → decrease of -8 % in the velocity

Table 4.3-1 - 6 mm plate velocity characteristics

Test#	Velocity [mm/min]		
Quality	#1.6	#2.6	#3.6
1	467,52	441,08	404,77
2	400,97	378,3	347,15
3	251,54	237,32	217,78
4	180,68	170,47	156,43
5	139,79	131,98	121,03

The velocity relation between all tests is the same during the three tests.

4.3.1.   Roughness Test

Table 4.3-2, Table 4.3-3 and Table 4.3-4 shows the average roughness values measured in the SRMI. The measurements were made on the top, middle and bottom surface, being the top position the closer to the entry point.

Table 4.3-2 - Ra values for test #1.6 mm

Pos tion	#1.6 [µm]		
Quality	Top	Middle	Bottom
1	4,8	6,8	>10
2	4,6	4,8	6
3	3,8	4,8	6
4	3,5	4,6	5
5	3,2	4,8	4,8

Table 4.3-3 - Ra values for test #2.6 mm

Position	#2.6 [µm]		
Quality	Top	Middle	Bottom
1	4,	5,2	6,6
2	3,8	4,8	6,6
3	3,6	4,8	5,5
4	3,6	4,6	4,8
5	3	4,2	4,2

Table 4.3-4 – Ra value for test #3.6 mm

#3.6 [μm]			
Position Quality	Top	Middle	Bottom
1	4,2	4,5	4,5
2	3	4,5	5
3	3,5	4,2	4,5
4	3	4	4,4
5	2,8	4	4,2

Those outliner results found on the 2 mm and 4 mm plate thick are no longer in this analysis. The R_a value increases in every test and for all positions, results shared by Hascalik, A. *et al*. (2007). The third test #3.6, quality 5 (slowest velocity in all test made 121.03 mm/min) has 2, 8 μm which is the lowest value in all test made.

In order to compare the roughness of surface cuts of the three tests, the evolution of roughness as function of the cutting speed is show in Fig 4.3-1, Fig 4.3-2 and Fig 4.3-3.
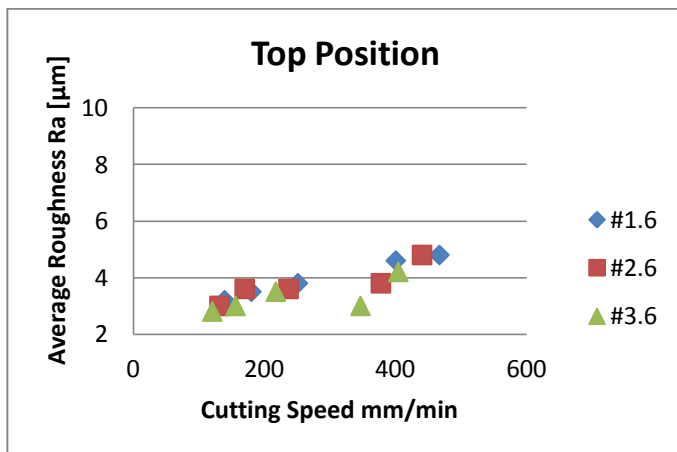
Fig 4.3-1 - Roughness Value Vs. Cutting speed on Top position. 6 mm plate thickness
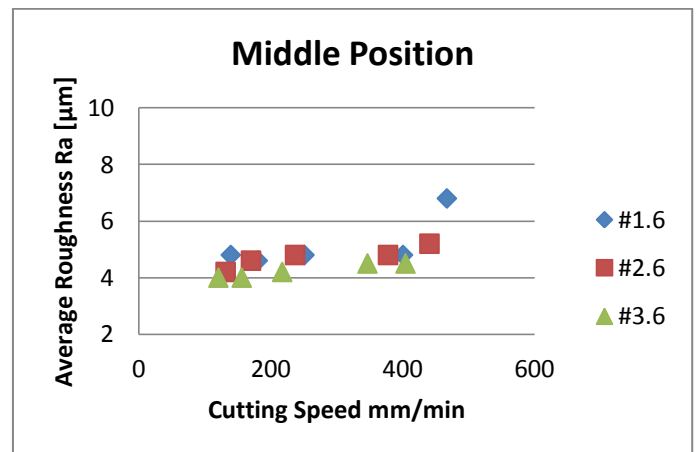
Fig 4.3-2 - Roughness Value Vs. Cutting speed on Middle position. 6 mm plate thickness
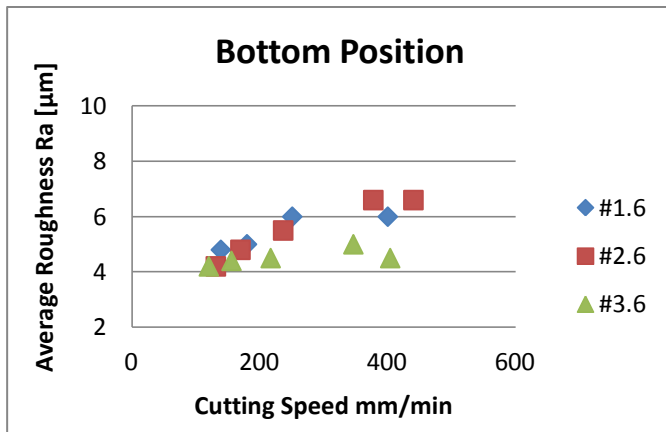
Fig 4.3-3 - Roughness Value Vs. Cutting speed on Bottom position. 6 mm plate thickness

All the three graphics Fig 4.3-1, Fig 4.3-2 and Fig 4.3-3 share the principal already argued, increasing the virtual thickness means better cutting surfaces. For test #3.6 (green points) the R_a value is the lowest in all three positions. Decreasing the cutting speed is a way to obtain lower R_a values, by consequence, better cutting surface. These results are in concordance with all the literature presented on the Reference chapter.

4.3.2.   Kerf Taper

The procedure was exactly the same as the one done for the 4 mm plate thick. The reference (1-5) and (6-10) refers to which set of faces are being analyzed.

- (1-5) - faces 1,2,3,4 and 5
- (6-10) - faces 6,7,8,9 and 10

Table 4.3-5 - Face Vs. Quality for 6 mm plate thick

Faces	Quality
1 and 6	5
2 and 7	4
3 and 8	3
4 and 9	2
5 and 10	1

The Fig 4.3-4 and Fig 4.3-5 refers to the Polyline strategy. In the Section C of the Appendix, there is the comparison between the "Polyline" and the "Without Polyline" strategy.
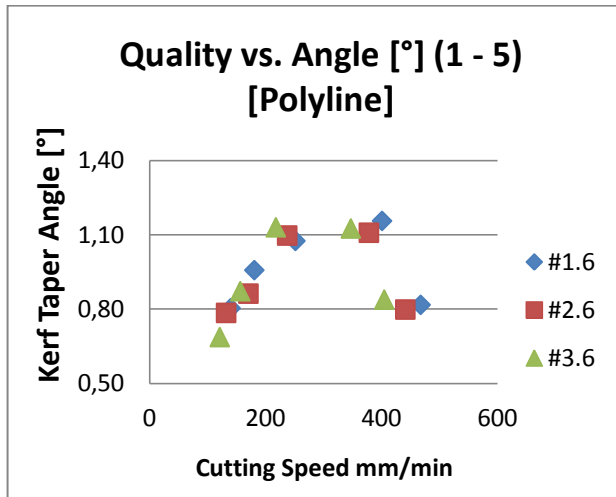
Fig 4.3-4 – Kerf Taper Angle Vs. Cutting speed. 6 mm plate, faces 1-5
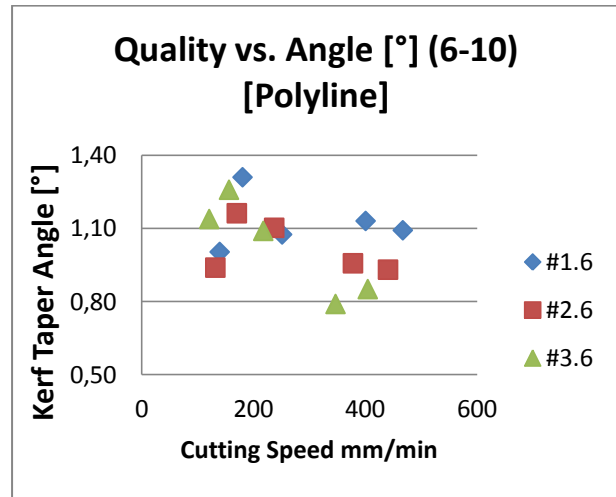
Fig 4.3-5 – Kerf Taper Angle Vs. Cutting speed. 6 mm plate, faces 6-10

The kerf taper angle given by the Fig 4.3-4 shows a common result, found on all graphic presented on this report regarding to the CMM analysis, the angle increases until a certain value. After that value, the angle is decreased by the increasing of cutting speed.

The Fig 4.3-5 presents an awkward result. None of the three test results fits on the profile presented in the earlier analysis.

Comparing all CMM graphic from all the tests made it is possible to withdrawn that slowing the cutting velocity, and by consequence having the jet more time to cut, produces smaller kerf taper angles. Another analysis can be made with the two set of faces, (1–5) and (6-10). The results presented in the first set of faces (1-5) are within the achieved results. This kind of measurement was not found on the literature, it was a new way to measure the taper angle.

4.3.3. Surface area

The presentation of the surface from the 6 mm plate thick will follow the guideline presented earlier for the 2 mm and 4 mm plate thick. Being a 6 mm plate thick, for the same magnifying lens, it was very difficult to capture the all surface and present a

picture where was clear the waviness of the surface. From the Table 4.3-2, Table 4.3-3 and Table 4.3-4, it is expected the cut surface to be the most perfect from all the 3 thicknesses. The red lines symbolize the trailback produced by the jet.

- First test #1.6. "virtual" thickness – 5 mm thick
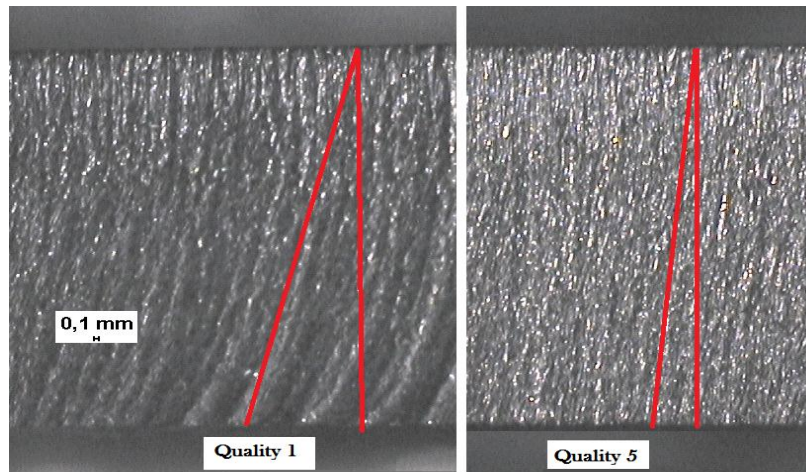
Fig 4.3-6 - Test #1.6. Quality 1 (467.52 mm/min) Vs. Quality 5 (139.79 mm/min)

Fig 4.3-6 shows the cut surface of quality 1 (467, 52 mm/min) and quality 5 (139, 79 mm/min) from the test #1.6. The waviness demonstrated in quality 1 is completely notorious and is a very good example of the jet path. Comparing both qualities is secure to say that by slowing the velocity, the trailback is decreased.

- Second test #2.6, real thickness – 6 mm thick
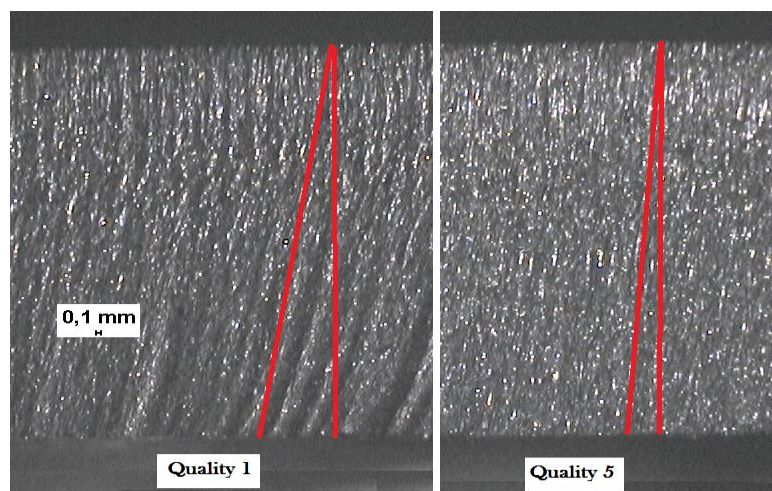
Fig 4.3-7 - Test #2.6. Quality 1 (441.08 mm/min) Vs. Quality 5 (131.98 mm/min)

Fig 4.3-7, quality 1 (441, 08 mm/min) and quality 5 (131, 98 mm/min), shows a trailback smaller than the Fig 4.3-6.

- Third test #3.6, "virtual" thickness – 7 mm thick
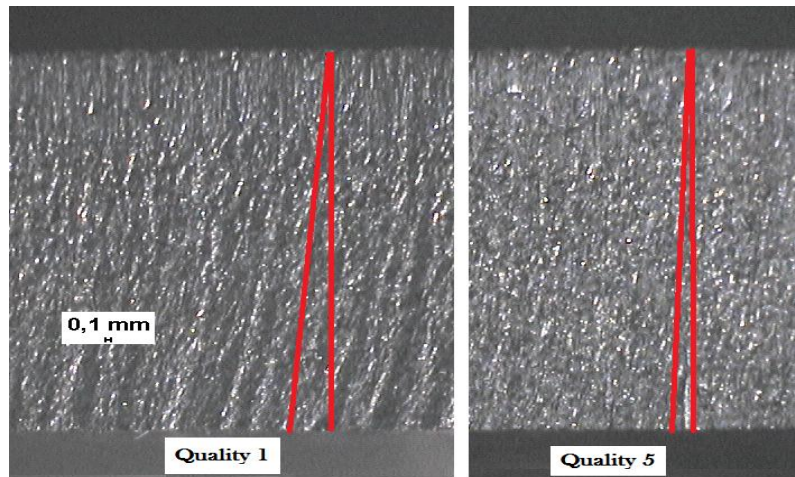
Fig 4.3-8 - Test #3.6. Quality 1 (404.77 mm/min) Vs. Quality 5 (121.03 mm/min)

The third test, see Fig 4.3-8, regarding to the slowest velocity from all test made, presents the most perfect cut surface corresponding to the quality 5 (121, 03 mm/min) R_a =2.8μm (top position) . The quality 1 (404, 77 mm/min) also presents a good cut surface, R_a = 4.2μm (top position).

From all the photos analyzed it is possible to conclude that the velocity has a major influence in the cut surface morphology. Despite the trailback have not been measure, Chen, F. L (2003) confirms the results found in all three plate thickness.

4.3.4.   Kerf Geometry

Top and bottom graphics are disposal next, comparing the distance between each side with the quality for the three specimens.
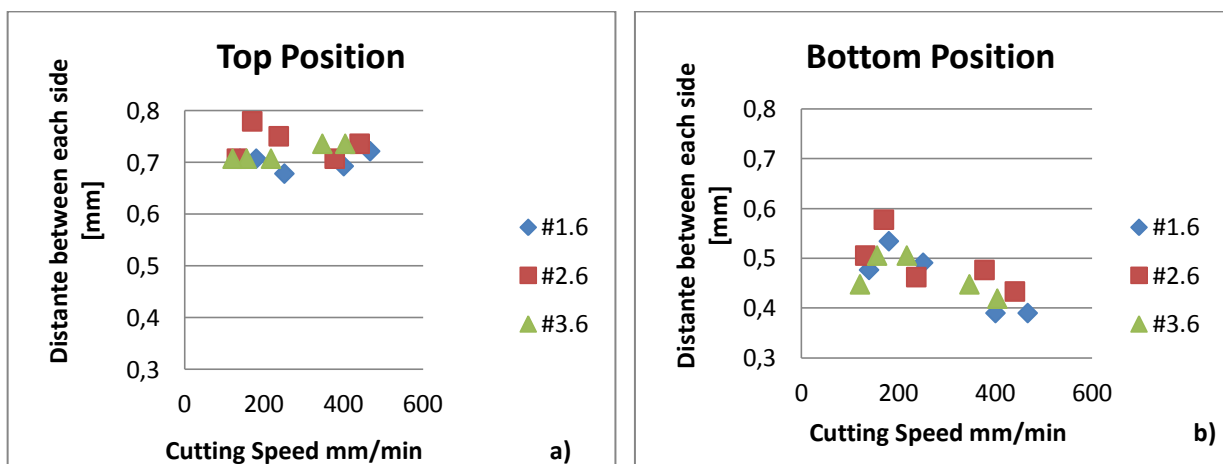
Fig 4.3-9 - Distance between each side of the cut. a) Top position; b) Bottom position

Like the graphic from Fig 4.1-8 a) (2 mm plate thick) the Fig 4.3-9 a) presents a lot of inconsistent results. The major amplitude differences between the highest and smallest distance value is 0, 0721 mm, and it is regarding to the #2.6 test. The graphic from Fig 4.3-9 b) shows the same characteristic as for the 2 mm and 4 mm plate thick, slowing the cutting speed the distance is increased. The trailback in this kind of thickness (6 mm thick), is higher than the one presented on the 2 mm and 4 mm plate thick.

Fig 4.3-10 shows a part of the back side from the test #1.6. As said earlier the outlines were cut with quality 3 (251.54 mm/min for the first test; 237.32 mm/min for the second test; 217.78 mm/min for the third test). As it is possible to see, the cut was incomplete, there were zones that were not cut, marked with the number 1 on the image.

Since the quality cuts were made first, when the beam is cutting the outline it has to pass through a "material gap", see Fig 4.3-11. The first part the jet in contact with that "material gap" is the entry point, the exiting point of the jet is still cutting a few milliliters behind. This difference leads to a jump, which result in not cutting the lowest part of the material. The grey area presented on the Fig 4.3-11 represents that fault.
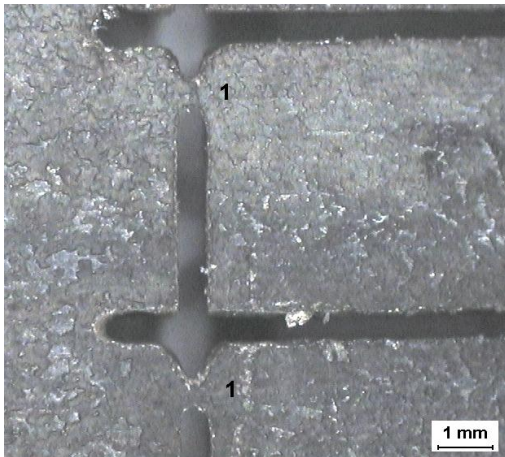
Fig 4.3-10 - Back side of #1.6 test
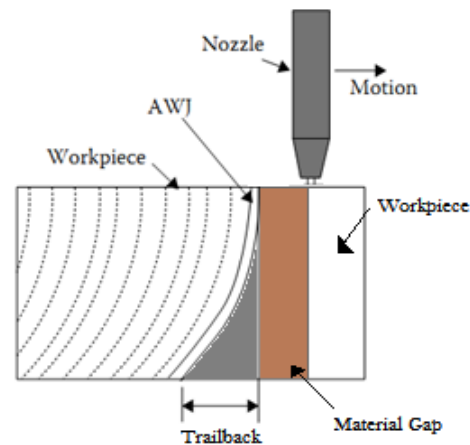
Fig 4.3-11 – Illustration of the failure produced by the "material gap"

4.4. Comparing test which have the same thickness

As said in the beginning of this chapter, results from the comparison between tests which have been cut with the same velocity but with different plate thickness will be presented. Roughness and kerf taper angle measurement results for each pair of workpieces cut with the same virtual thickness will be presented during the following chapter. Those tests are:

- #3.2 with #1.4 – assuming a virtual thickness of 3 mm;
- #3.4 with #1.6 – assuming a virtual thickness of 5 mm;
- #4.4 with #2.6 – assuming a virtual thickness of 6 mm.

4.4.1.   Virtual thickness of 3 mm

The two plates 2 mm (test #3.2) and 4 mm (test #1.4) were cut as assuming a virtual thickness of 3 mm. Table 4.4.1-1, given by the MAKE program, combines the cutting velocity with the correspondent quality.

Table 4.4.1-1 – Cutting velocity Vs. Quality for the 3 mm thick

Quality	Ideal Linear Velocity [mm/min]
1	724,34
2	621,23
3	398,71
4	279,94
5	216,58

4.4.1.1. Roughness Test

The roughness in top and bottom position is shown in Fig 4.4.1-1 and Fig 4.4.1-2, respectively.
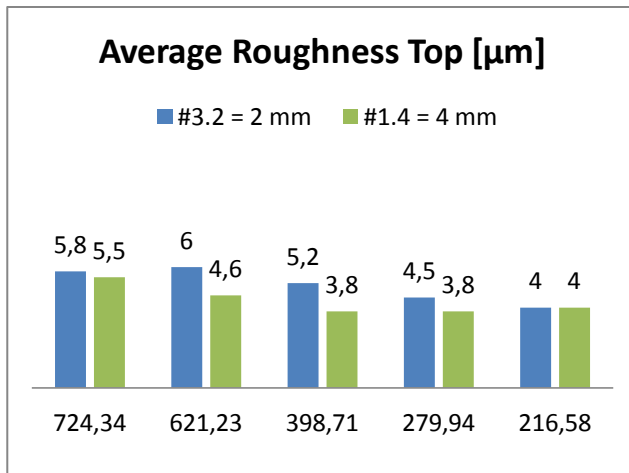
Fig 4.4.1-1 - Roughness Value Vs. Cutting speed on Top position
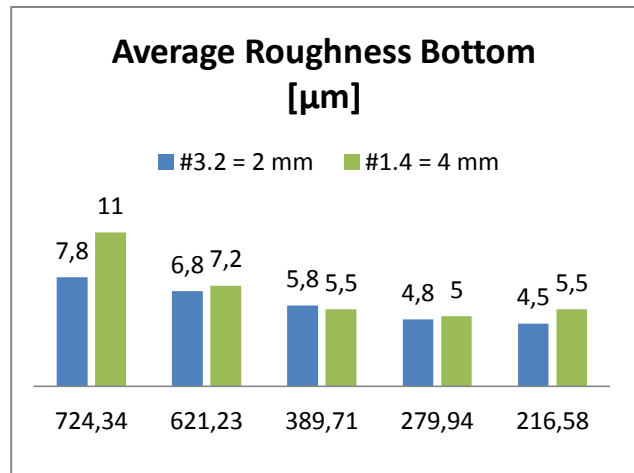
Fig 4.4.1-2 - Roughness Value Vs. Cutting speed on Bottom position

Fig 4.4.1-1 and Fig 4.4.1-2 shows two different results. On the top position, the test #1.4 = 4 mm thick presents smoother surface comparing to the #3.2 = 2 mm thick. On the second graphic, bottom position, it is the other way around. The test #3.2 = 2 mm is the one who presents the smoother surface. The two tests were not programmed according to their real thickness, which means that for the 2 mm the cut was more than enough, in the 4 mm thick case, the cut was programmed above the real thickness. On top position those differences are not clear, but for the bottom position, is clear the lack of beam power on the 4 mm thick, resulting in the smoother cut surface of the 2 mm thick on bottom position.

4.4.1.2. Kerf Taper

Fig 4.4.1-3 gives the kerf taper angle relation between the 2 mm thick and the 4 mm thick plate with the cutting speed. The graphic above have three colours for two thicknesses, since the 2 mm plate only have one set of faces and the 4 mm thick plate have two set of faces (1-5) and (6-10).
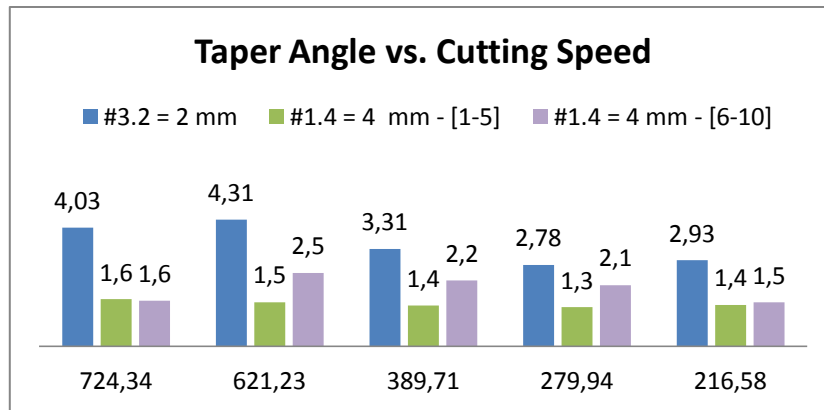
Fig 4.4.1-3 – Kerf taper angle vs. cutting speed, according to the CMM

Fig 4.4.1-3 shows that the 2 mm plate thick, presents for all qualities, the highest kerf taper angle. For the same velocity the smallest thickness presents the highest angle, in this case the 2 mm plate thick.

4.4.2.   Virtual thickness of 5 mm

The two plates 4 mm (test #3.4) and 6 mm (test #1.6) were cut as assuming a virtual thickness of 5 mm. Table 4.4.2-1 given by the MAKE program, combines the cutting speed with the correspondent quality.

Table 4.4.2-1 – Cutting velocity Vs. Quality for the 5 mm thick

Quality	Ideal Linear Velocity [mm/min]
1	467,52
2	400,97
3	251,54
4	180,68
5	139,79

4.4.2.1.   Roughness Test

The roughness at top and bottom positions is shown in Fig 4.4.2-1 and Fig 4.4.2-2, respectively.

Average Roughness Top [μm]

■ #3.4 = 4 mm   ■ #1.6 = 6 mm

| | 4 | 4,8 | 4 | 4,6 | 3,8 | 3,8 | 3,5 | 3,5 | 3,2 | 3,2 |

467,52   400,97   251,54   180,68   139,79

Average Roughness Bottom [μm]

■ #3.4 = 4 mm   ■ #1.6 = 6 mm

6,2   11   5,5   6   4,8   6   5   5   4   4,8

467,52   400,97   251,54   180,68   139,79
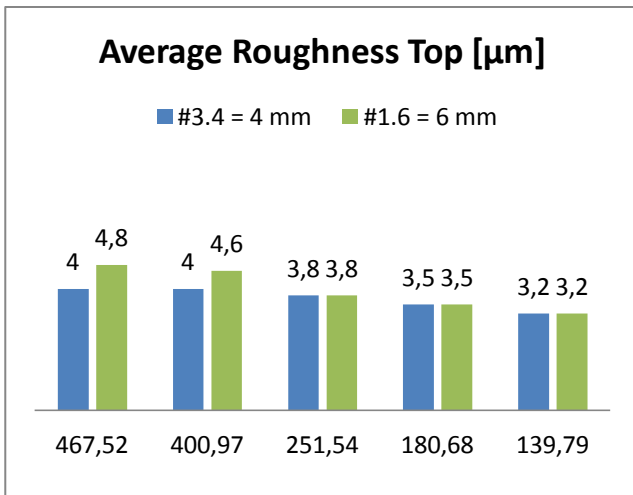
Fig 4.4.2-1 - Roughness value Vs. Cutting speed on top position
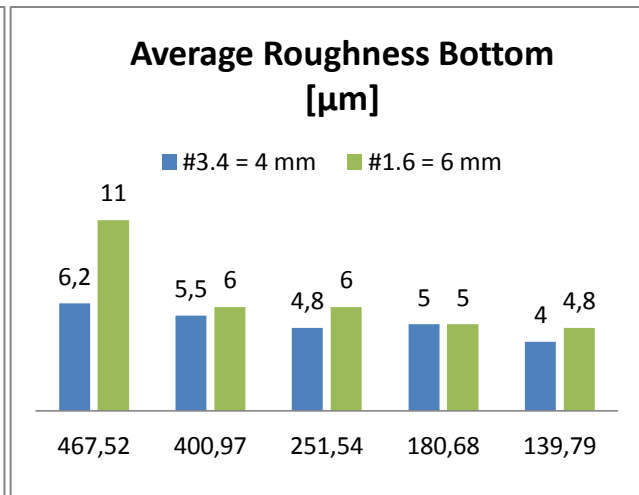
Fig 4.4.2-2 - Roughness value Vs. Cutting speed on Bottom position

The analysis made for the previous pair of test become more sustainable with these results. The 6 mm plate thick presents higher R_a value both top and bottom position and because of that, worst cut surface. The hypothesis present previous becomes valid, for the same velocity the thickest plate presents worst cut surface on top and on bottom.

4.4.2.2.   Kerf Taper

Fig 4.4.2-3 and Fig 4.4.2-4 gives the kerf taper angle in both set of faces, relation between the 4 mm plate thick and the 6 mm thick plate with the cutting speed. The two plates were evaluated in all the ten faces (two sets of faces). The Fig 4.4.2-3 gives the results of the first set of faces (1-5) and the Fig 4.4.2-4 the second set of faces (6-10).

Taper Angle vs. Cutting Speed (1 - 5)

■ #3.4 = 4 mm   ■ #1.6 = 6 mm

1,4   1,01   1,7   1,14   1,4   1,07   1,6   1,12   1,4   0,85

467,52   400,97   251,54   180,68   139,79

Taper Angle vs. Cutting Speed (6 - 10)

■ #3.4 = 4 mm   ■ #1.6 = 6 mm

1,7   0,77   2,0   1,11   1,8   0,99   1,6   0,90   1,1   0,80

467,52   400,97   251,54   180,68   139,79
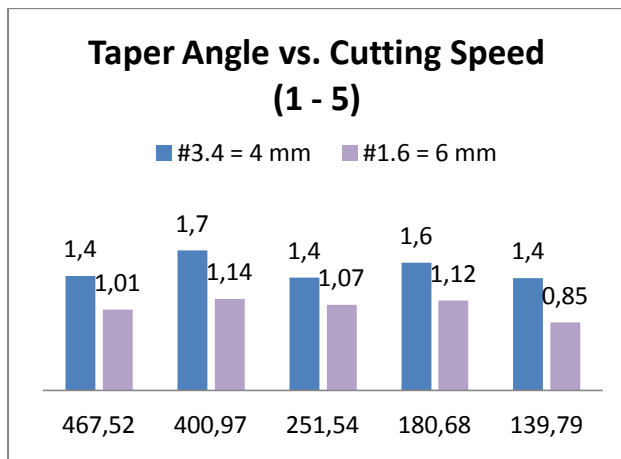
Fig 4.4.2-3 – CMM result for the first set of faces (1-5)
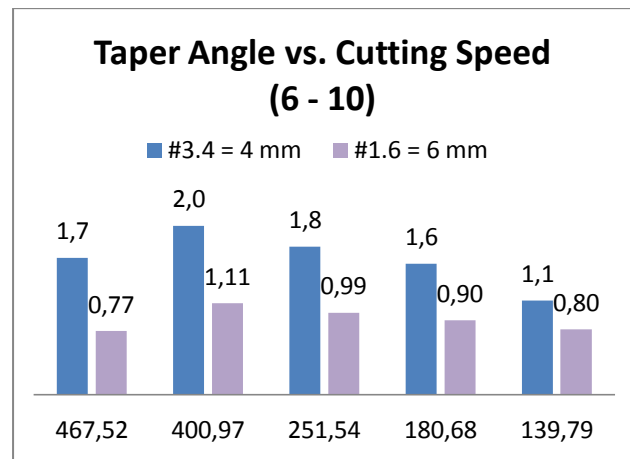
Fig 4.4.2-4 - CMM result for the second set of faces (6-10)

In both figures, Fig 4.4.2-3 and Fig 4.4.2-4 the 6 mm plate thick presents the smallest kerf taper angle, in concordance with the previous analyzes.

4.4.3.   Virtual thickness of 6mm

This third pair for analysis is with the same plate thicknesses as the previous pair. The two plates 4 mm (test #4.4) and 6 mm (test #2.6) were cut as assuming a virtual thickness of 6 mm. Table 4.4.3-1, given by the MAKE program, combines the cutting speed with the correspondent quality.

Table 4.4.3-1 -Cutting velocity Vs. Quality for the 6 mm thick

Quality	Ideal Linear Velocity [mm/min]
1	441,08
2	378,3
3	237,32
4	170,47
5	131,89

4.4.3.1.   Roughness Test

The roughness at top and bottom positions is shown in Fig 4.4.3-1 and Fig 4.4.3-2 respectively.

Average Roughness Top [μm]
■ #4.4 = 4 mm   ■ #2.6 = 6 mm

| 441,08 | 378,3 | 237,32 | 170,47 | 131,98 |

Fig 4.4.3-1 - Roughness value Vs. Cutting speed on Top position

Average Roughness Bottom [μm]
■ #4.4 = 4 mm   ■ #2.6 = 6 mm

| 441,08 | 378,3 | 237,32 | 170,47 | 131,98 |
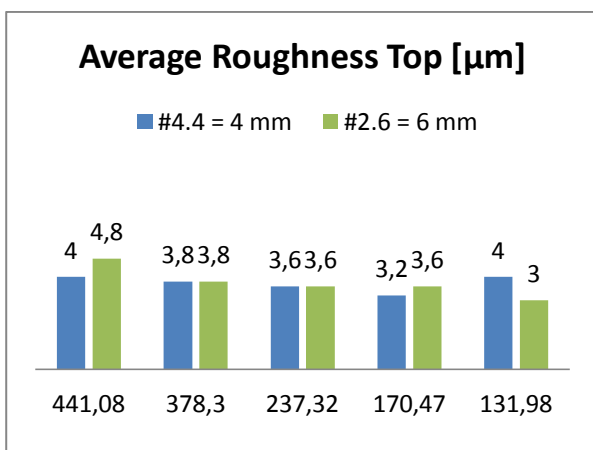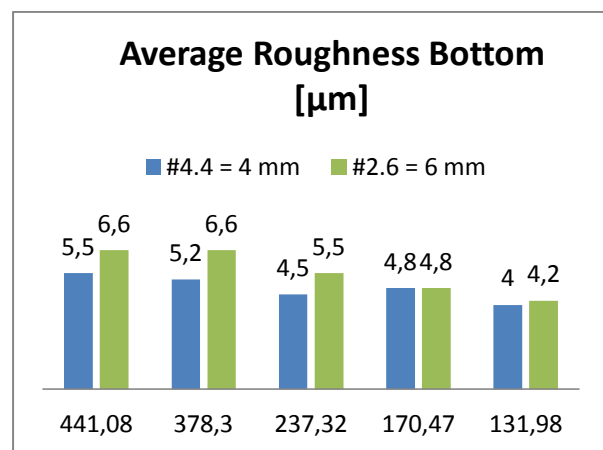
Fig 4.4.3-2 - Roughness value Vs. Cutting speed on Bottom position

Once more, the Roughness comparison gives the same results, thinner workpiece smoother surface.

In a global way, for the same cutting velocity, the R_a values are higher for higher plate thicknesses.

4.4.3.2. Kerf Taper

Fig 4.4.3-3 and Fig 4.4.3-4 gives the kerf taper angle in both set of faces, relation between the 4 mm plate thick and the 6 mm thick plate with the cutting speed. The presentation is the same made for the 5 mm thickness, previously made.
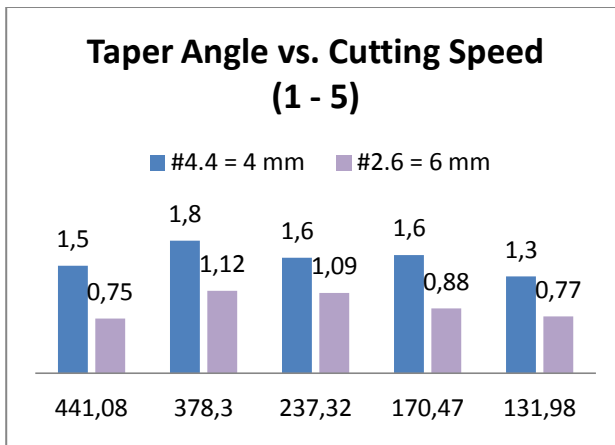
Fig 4.4.3-3 - CMM result for the first set of faces (1-5)
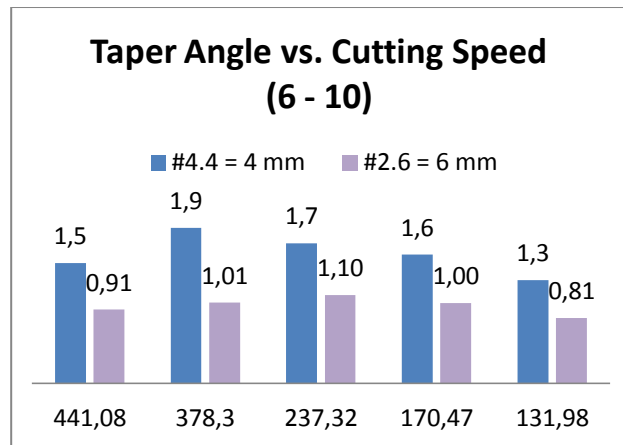
Fig 4.4.3-4 - CMM result for the second set of faces (6-10)

Both figures, Fig 4.4.3-3 and Fig 4.4.3-4 fortify the principle that thinner the workpiece, for the same velocity, higher the kerf taper angle is.

The CMM analysis, for all tests made (3 mm, 5 mm and 6 mm), gives the same result. The 2 mm plate thick presents highest kerf taper angle than the 4 mm plate thick, cut with the same velocity. The same approach can be made when comparing the 4 mm with the 6 mm plate thick.

This kind of comparison was not found in the literature gathered for this experimental work. I personally believe is of great importance analyzing the differences in cut surface for plates cut with same velocity but which have different plate thicknesses.

5. Conclusions

In this study surface roughness, perpendicularity planes and kerf geometry of water jet cutting surfaces as function of traverse speed and plate thickness were empirically investigated. From the main results presented above, the following conclusions can be drawn:

1. Roughness of cut surface increases with increasing cutting speed and plate thickness;

2. The kerf taper angle decreases with decreasing cutting speed;

3. The thinner the workpiece, the better the cut surface but the bigger the kerf taper angle.

4. The decrease in cutting speed produces larger distances on top and on bottom of the cuts. The distance between the entry and exiting points of the jet decreases with the reduction of cutting speed (trailback);

Cutting in a "material gap" may produce defect on the surface also the support bars damage the bottom workpiece surface mainly because of the jet deflection.

The most noticeable conclusion withdrawn from the experimental work is the fact that the average roughness, kerf taper angle and kerf width values behave the same way whether for the plate of 2 mm, 4mm or 6 mm thick. The behaviour of cutting speed parameters is the same for the 3 plate thicknesses.

The former are the collected conclusions from the results presented in the chapter 4. There are also other conclusions that can be drawn from the experiments carried out with the material and the machines, which will be addressed next.

The approach made for the taper angle analysis, with the CMM machine, proved to be accurate.

Despite the problems found in the SRMI measurements, the Ra values collected are in general agreement with the literature surveyed.

If the waterjet machine is idle for a long period of time (typically 48 hours), it takes a few seconds running by itself for cleaning any abrasive aggregation that could be

either inside the nozzle or the mixing tube; this kind of abrasive aggregation can produce defects.

Another problem was the placement of the steel plates on top of the supporting bars. The waterjet machine does not have a clamping system therefore an archaic method had to be used.

Oxidation is present during the whole process, due to the water contact with the metal. When visualizing the cut surface with increased precision, for instance with a microscope lens, the corrosion induced by the exposure to water is enhanced.

6. Future Work

In this work, the effect of two parameters, the cutting speed and the plate thickness on the quality of waterjet cuttings were studied. However, the process is also influenced by other important parameters that require additional research, of which the following are worth mentioning and studying:

- To change the abrasive feed rate and/or abrasive size, and analyze their influence on the surface quality;
- To change the water pressure;
- To use the tilt jet to minimize the taper;
- Expand the metrics collection by analyzing the cut surface roughness not only with the R_a value but also with R_q, R_t, R_p, R_v and R_y;
- Cut more work pieces with the same "virtual thickness" in order to allow statistical analysis of the results.

7. References

Akkurt, A., Kulekci, M., K., Seker, U., Ercan, F. (2004), "Effect of feed rate on surface roughness in abrasive waterjet cutting applications", Journal of Materials Processing Technology, 147, 389–396

Hascalik, A., Caydas, U., Gurun, H. (2007), "Effect of traverse speed on abrasive waterjet machining of Ti–6Al–4V alloy", Materials and Design, 28, 1953–1957

Antunes, N. C. A. (2011), "Cutting of carbon fiber reinforced polymer using abrasive water jet technology", Master thesis in Mechanical Engineering, University of Coimbra

Shanmugam, D. K., Chen F.L., Siores, E., Brandt, M. (2002), "Comparative study of jetting machining technologies over laser machining technology for cutting composite materials", Composite Structures, 57, 289–296

Shanmugam, D. K., Wang, J., Liu, H. (2008), "Minimization of kerf tapers in abrasive waterjet machining of alumina ceramics using a compensation technique", International Journal of Machine Tools & Manufacture 48 (2008) 1527–1534

Shanmugan, D. K., Masood, S. H. (2009), "An investigation on kerf characteristics in abrasive waterjet cutting of layered composites", journal of materials processing technology, 209, 3887–3893

Ness, E., Zibbell, R., (1996), " Abrasion and erosion of hard materials related to wear is abrasive waterjet", Wear, 196, 120-125

Chen, F.L., Wangb, J., Lemmaa, E., Siores, E. (2003), "Striation formation mechanisms on the jet cutting surface", Journal of Materials Processing Technology, 141, 213–218

Zheng, H.Y., Han, Z.Z., Chen, X.D., Yeo, S. (1996), "Quality and Cost Comparison between Laser and Waterjet Cutting", Journal of Materials Technology, 62, 294-298

http://www.barton.com, 06/07/2011

http://www.flowwaterjet.com, 22/07/2011

http://www.minerals.net, 15/07/2011

http://www.omax.com, 06/07/2011

http://www.preved.com, 08/07/2011

http://www.zaporizhstal.com, 016/07/2011

http://www.zeiss.com/, 06/06/2011

Wang, J. and Wong, W. C. K. (1999), "A study of abrasive waterjet cutting of metallic coated sheet steels", International Journal of Machine Tools & Manufacture, 39, 855–870

Oliveira Santos, F. J., Quintinho, L., Miranda, R. M., ISQ, (1991), "Processamento de materiais por feixe de electrões, laser e jacto de água", Edições Tecnicas do Instituto de Soldadura e Qualidade.

Valıceka, J., Drzıkb, M., Hlochc, S., Ohlıdal, M., Miloslave, L., Gombar, M., Radvanskag, A., Hlavacekh, P., Palenıkova, K. (2007), "Experimental analysis of irregularities of metallic surfaces generated by abrasive waterjet", International Journal of Machine Tools & Manufacture, 47, 1786–1790

Folks, J. (2009), "Water jet – An innovative tool for manufacturing", Journal of Materials Processing technology, 209, 6181-6189

Wang, J. (1999), "A machinability study of polymer matrix composites using abrasive waterjet cutting technology", Journal of Materials Processing Technology, 94, 30–35

Hashish, M. (2011), "Energy Fields in Waterjet Machining", In Zhang, W. (ed), Intelligent Energy Field Manufacturing, CRC Press, 141-171

Gudimetla, P., Wang, J., Wong, W. (2002), " Kerf formation analysis in the abrasive waterjet cutting of industrial ceramics", Journal of Materials Processing Technology, 128, 123–129

8. Appendix

In this chapter the comparison between "Polyline" and "Without Polyline" technique will be presented for all test made in Section A to C and also data references that complements the carried out study.

Section A will be for the 2 mm plate thick, Section B for the 4 mm plate thick and Section C for the 6 mm plate thick.
 In Section D there are the two paper record regarding to the SRMI.

A. 2 mm plate thick

Fig A-1, Fig A-2 and Fig A-3 shoes the kerf taper angle results for the test #1.2, #2.2 and #3.3, respectively.
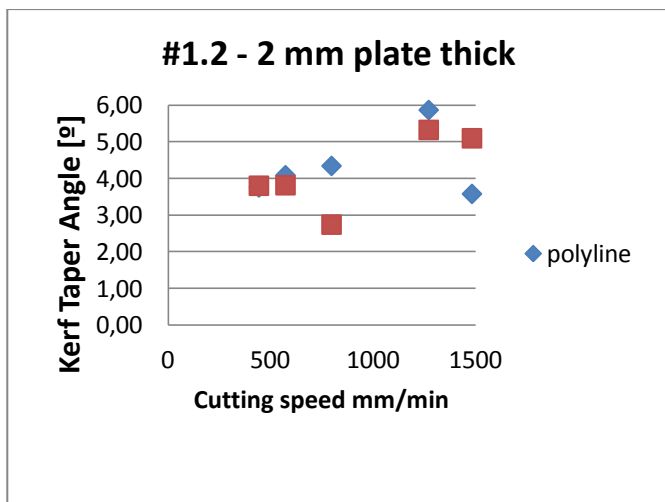
Fig A-1 – Comparing the two techniques on the #1.2 test
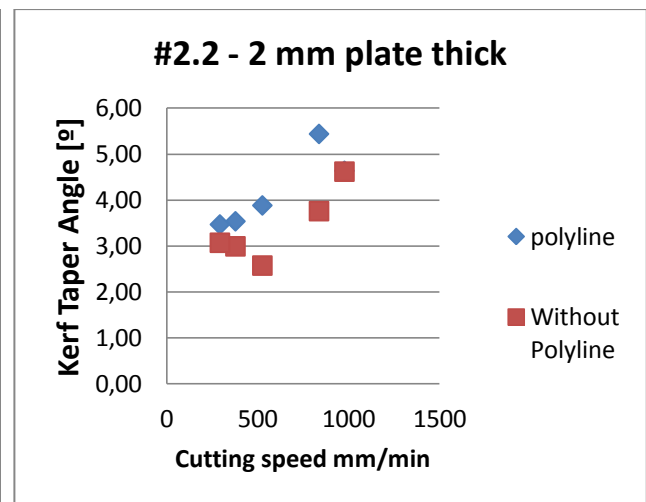
Fig A-2 - Comparing the two techniques on the #2.2 test
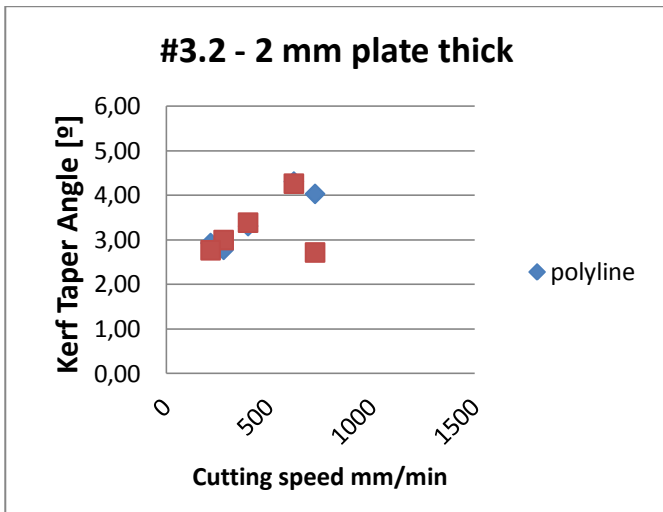
Fig A-3 - Comparing the two techniques on the #3.2 test

Fig A-1 and Fig A-3 does not transmit a strong position relatively to which technique is better to use. Fig A-2 shows for all qualities that the "Polyline" strategy gives the highest kerf taper values.

B.   4 mm plate thick

Section B a) presents the kerf taper angle results for the first set of faces (1-5) and Section B b) the results for the second set of faces (6-10).

a)   First set of Faces 1 to 5

Fig B-1,

Fig B-2, Fig B-3 and Fig B-4 shows the kerf taper angle results for the test #1.4, #2.4, #3.4 and #4.4, respectively.
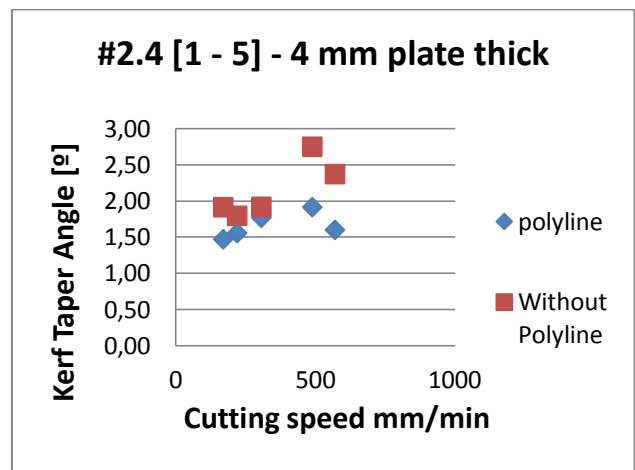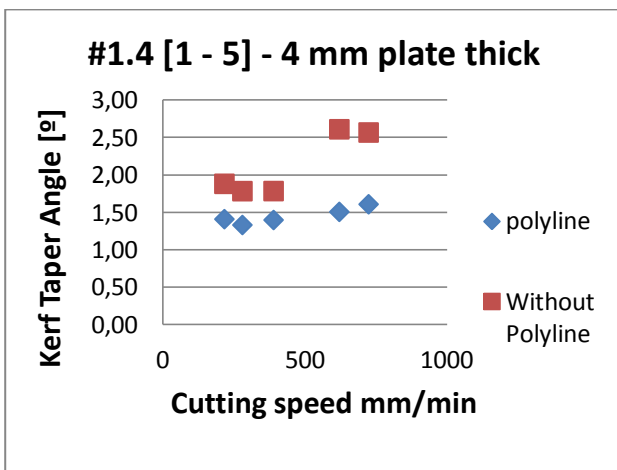
Fig B-1 - Comparing the two techniques on the # 1.4 test. First set of faces (1-5)

Fig B-2 - Comparing the two techniques on the # 2.4 test. First set of faces (1-5)
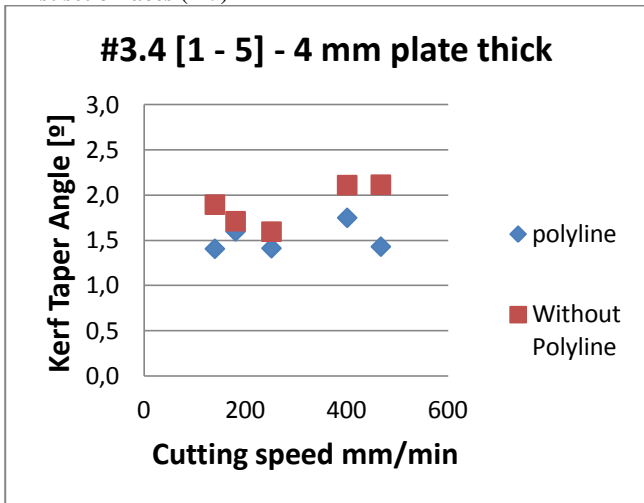
Fig B-3 - Comparing the two techniques on the # 3.4 test. First set of faces (1-5)
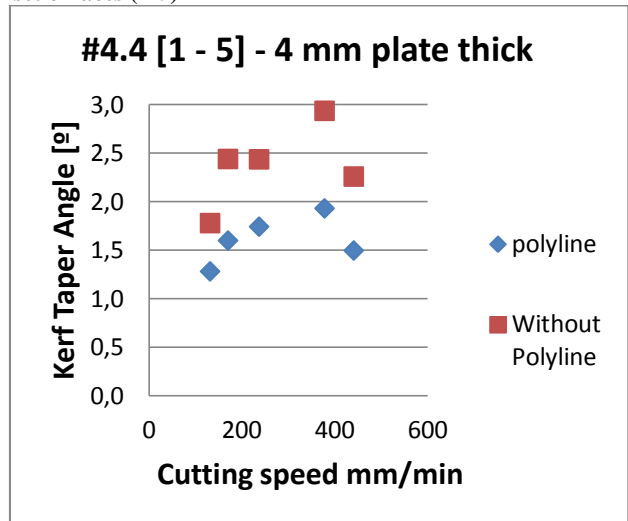
Fig B-4 - Comparing the two techniques on the # 4.4 test. First set of faces (1-5)

b)   Second set of Faces 6 to 10

Fig B-5, Fig B-6, Fig B-7 and Fig B-8 shows the kerf taper angle results for test #1.4, #2.4, #3.4 and #4.4, respectively.
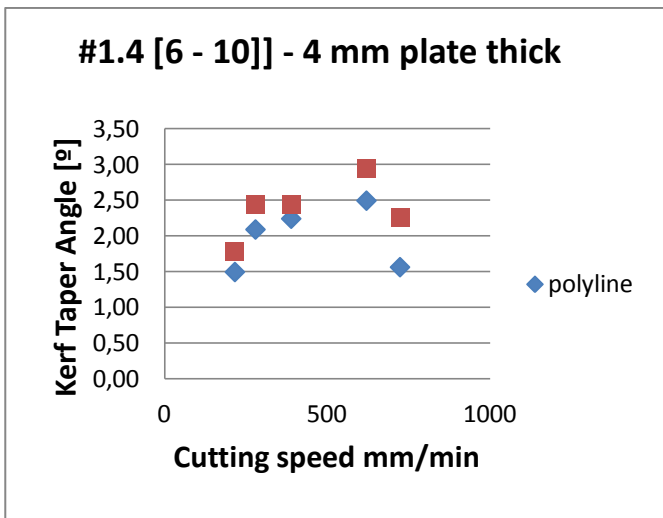
Fig B-5 - Comparing the two techniques on the # 1.4 test. Second set of faces (6-10)
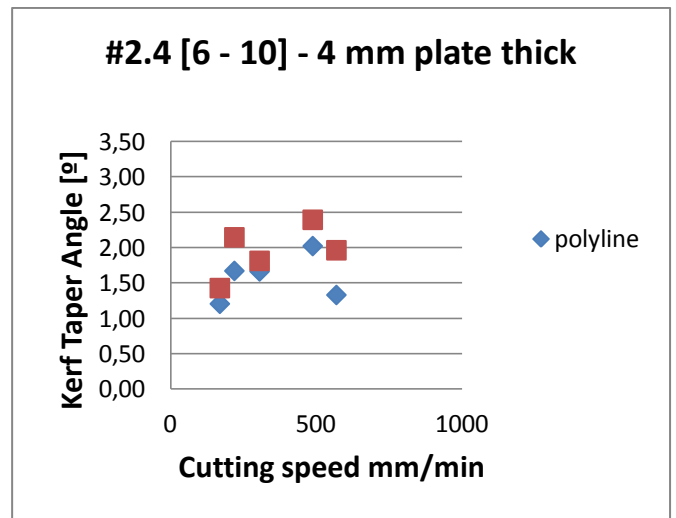
Fig B-6 - Comparing the two techniques on the # 2.4 test. Second set of faces (6-10)
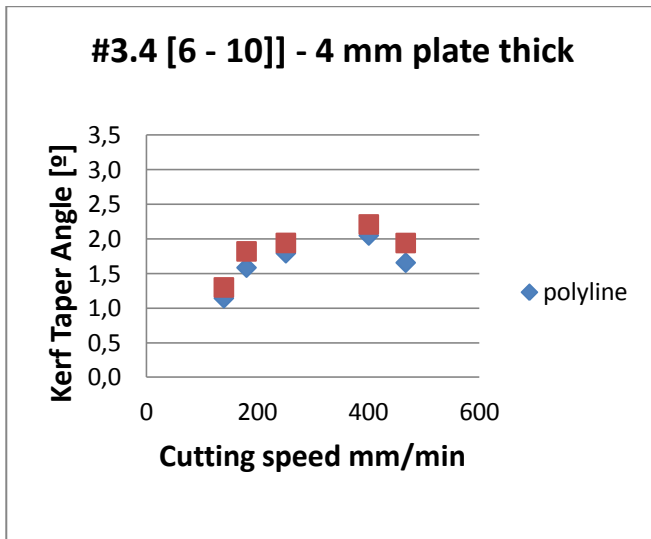
Fig B-7 - Comparing the two techniques on the # 3.4 test. Second set of faces (6-10).
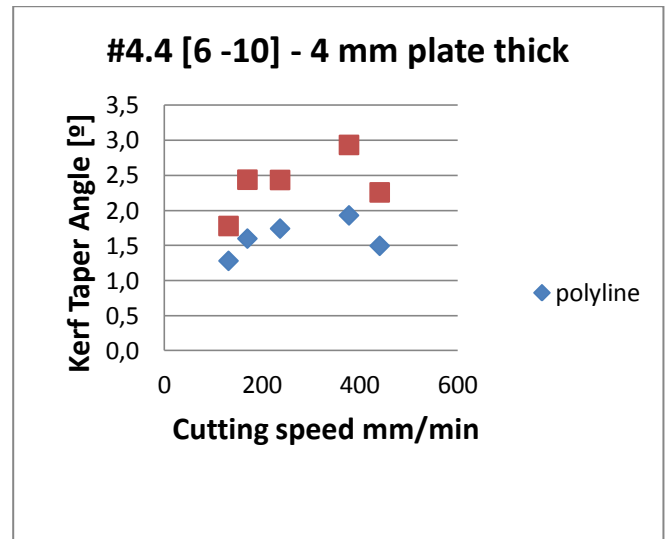
Fig B-8 - Comparing the two techniques on the # 4.4 test. Second set of faces (6-10)

Either the first set or the second set of faces gives the same result; the "Polyline" technique presents the smallest kerf taper angle. This result was expected since the Polyline technique uses about 90 points and can produce a more reliable surface plane.

C.   6 mm plate thick

Section C a) presents the kerf taper angle results for the first set of faces (1-5) and Section C b) the results for the second set of faces (6-10).

a)   First set of Faces 1 to 5

Fig C-1, Fig C-2 and Fig C-3 shows the kerf taper angle results for test #1.6, #2.6 and #3.6, respectively.
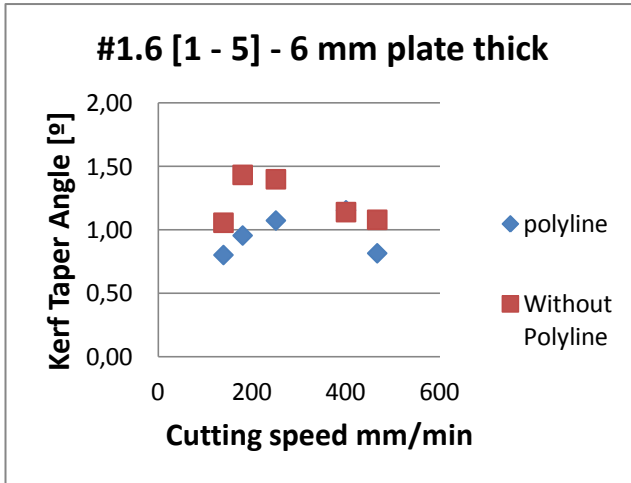
Fig C-1 - Comparing the two techniques on the # 1.6 test. First set of faces (1-5)
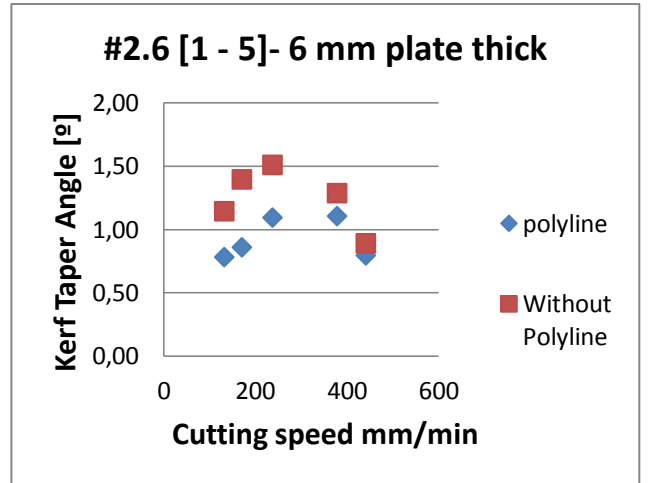
Fig C-2 - Comparing the two techniques on the # 2.6 test. First set of faces (1-5)
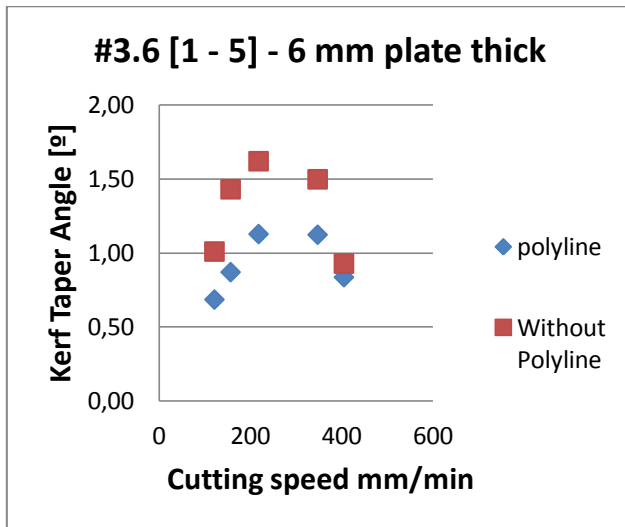
Fig C-3 - Comparing the two techniques on the # 3.6 test. First set of faces (1-5)

b)   Second set of Faces 6 to 10

Fig C-4, Fig C-5 and Fig C-6 shows the kerf taper angle results for test #1.6, #2.6 and #3.6, respectively.
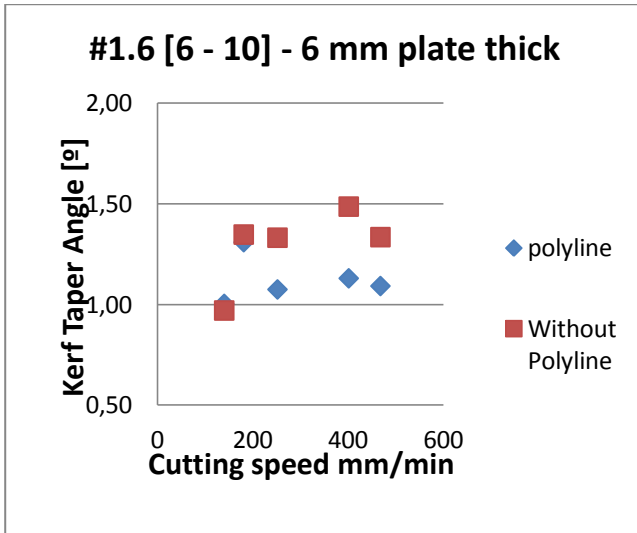
Fig C-4 - Comparing the two techniques on the # 1.6 test. Second set of faces (6-10)
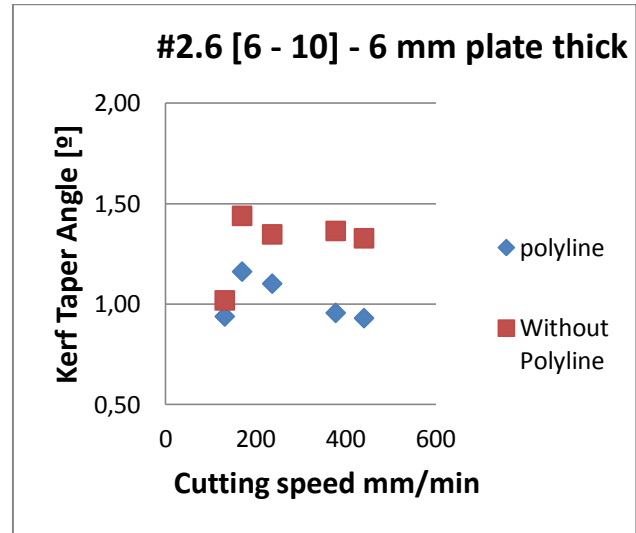
Fig C-5 - Comparing the two techniques on the # 2.6 test. Second set of faces (6-10)
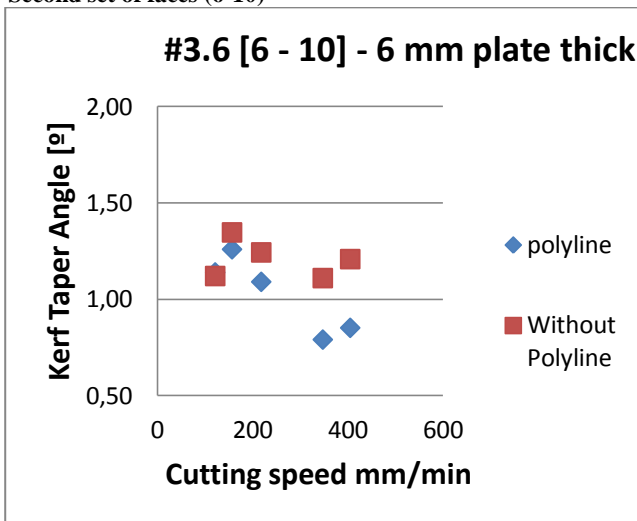
Fig C-6 – Comparing the two techniques on the # 3.6 test. Second set of faces (6-10)

Analysing all graphic, the Fig C-1 on the quality 2 and Fig C-6 on the quality 5 are the only values that the "Without Polyline" technique presents better results over the "Polyline" technique. All the other results are according to the expected, the "Polyline" presents smaller kerf taper angle than the "Without Polyline" technique.

D.   Paper record

As said before, SRMI allows us keep a graphic paper record, from the cut surface that we are being analyzed. Fig D-1 and Fig D-2 represent the top, middle and bottom position, respectively. Top position was measured with 20 times, middle and

bottom position with normal way N, they shows the cut surface from the 6 mm plate thick in two test, #1.6 – with the worst quality, and #3.6 - with the best quality.
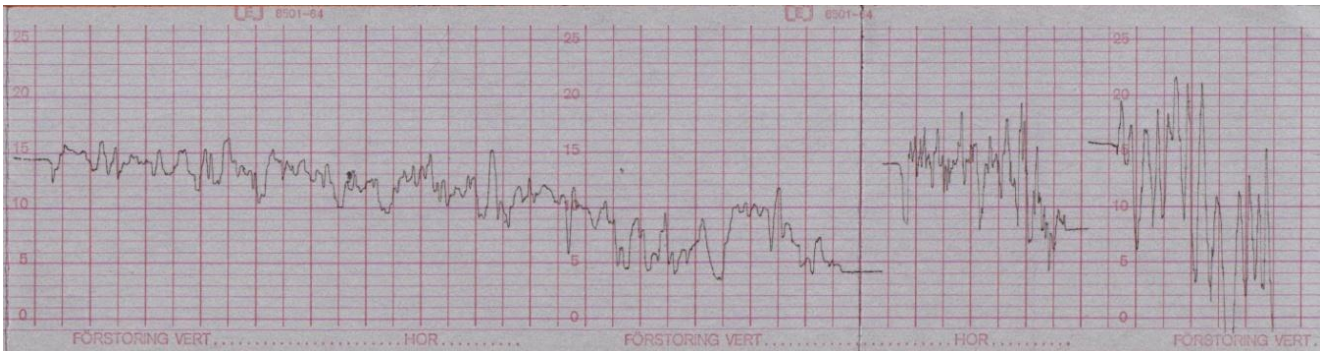
Top	Middle	Bottom

Fig D-1 – Paper record from test # 1.6. Quality 1 (467.52 mm/min)
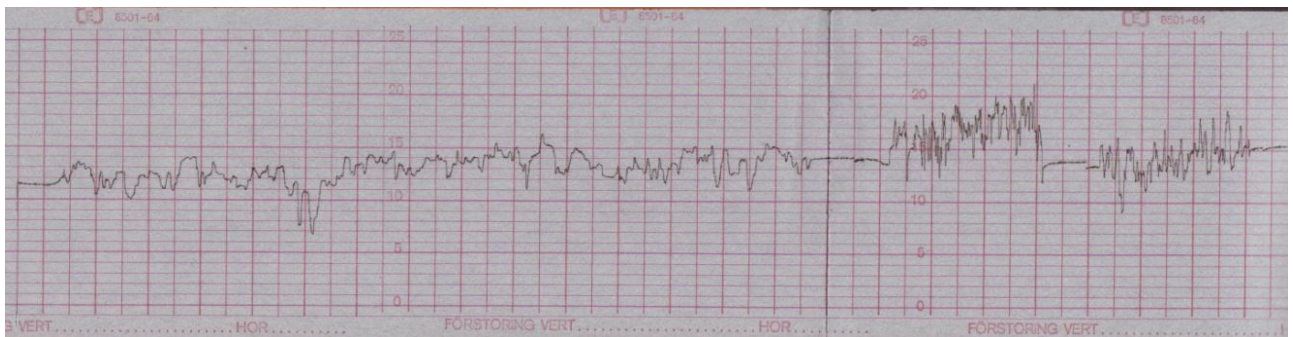
Top	Middle	Bottom

Fig D-2 - Paper record from test # 3.6. Quality 5 (121.03 mm/min)

It is notorious the difference between them. The most impressive difference is the bottom graphic.